Table 5.6 Units Used with Radiation Exchange Equation

Item	Symbol	English Units	Metric Units
Radiant heat exchange	Q	$\frac{\text{Btu}}{\text{hr}}$	$\frac{\text{cal}}{\text{sec}}$
Stefan–Boltzmann constant	σ	$\frac{0.1713 \times 10^{-8}\ \text{Btu}}{\text{hr ft}^2\ {}^\circ\text{R}^4}$	$\frac{1.355 \times 10^{-12}\ \text{cal}}{\text{sec cm}^2\ {}^\circ\text{K}^4}$
View factor	f	Dimensionless	Dimensionless
Emissivity	e	Dimensionless	Dimensionless
		$\frac{1}{1/e_1 + 1/e_2 - 1}$	$\frac{1}{1/e_1 + 1/e_2 - 1}$
Area	A	ft^2	cm^2
Absolute temperature	T	°F + 460 = °R	°C + 273 = °K

The finned surface increases the effective area for convection heat transfer but has very little affect on the effective area for radiation heat transfer. Radiating surfaces must be able to "see" each other in order to transfer heat. The fins block the line of sight so that only the projected area bounded by the tight string is effective for the transfer of heat.

5.17 RADIATION VIEW FACTOR

The view factor f is defined as the fraction of the radiation leaving surface 1 in all directions, which is intercepted by surface 2, as shown in Figure 5.17.

Heat transferred by radiation can be evaluated as taking place from surface 1 to surface 2, or from surface 2 to surface 1, if both are black bodies, whichever is more convenient. The product of the area times the

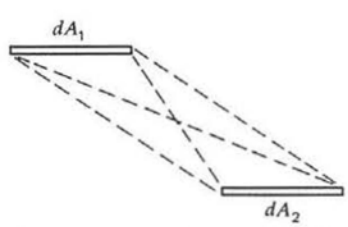

Figure 5.17 Areas involved in a radiation interchange.

SEC et al. v. MRI
SEC Exhibit 1027.0151
IPR2023-00255

view factor works in both directions, as shown in Eq. 5.48 [15, 24].

$$A_1 f_{1-2} \equiv A_2 f_{2-1} \tag{5.48}$$

Many complex equations have been derived, and many computer programs are available, which relate the view factor between two surfaces as a function of the geometry. Sometimes it is possible to determine the view factor between two rectangular plates with a piece of string, using the cross string method.

For example, consider two long, narrow, rectangular parallel plates as in Figure 5.18, where only the narrow edges are shown. Using a piece of string, the dimensions across the free edges are shown by the dashed lines.

As shown by Eq. 5.48, the product of the area times the view factor, per unit length of depth, is the sum of the lengths of the crossed strings stretched from the edges of the plates, minus the sum of the lengths of the noncrossed strings similarly stretched from the edges of the plates, all divided by 2. This is shown as follows:

$$A_1 f_{1-2} = A_2 f_{2-1} = \frac{\text{sum cross strings} - \text{sum noncross strings}}{2} \tag{5.49}$$

$$A_1 f_{1-2} = A_2 f_{2-1} = \frac{(8.54 + 5.0) - (5.0 + 3.0)}{2} = 2.77 \frac{\text{in}^2}{\text{in of depth}}$$

The view factor from plates 1 to 2 (f_{1-2}) is

$$f_{1-2} = \frac{A_2 f_{2-1}}{A_1} = \frac{2.77 \text{ in}^2/\text{in}}{(4)(40) \text{ in}^2}(40 \text{ in}) = 0.692 \text{ (dimensionless)} \tag{5.50}$$

The view factor from plates 2 to 1 (f_{2-1}) is

$$f_{2-1} = \frac{A_1 f_{1-2}}{A_2} = \frac{2.77 \text{ in}^2/\text{in}}{(8)(40) \text{ in}^2}(40 \text{ in}) = 0.346 \text{ (dimensionless)} \tag{5.51}$$

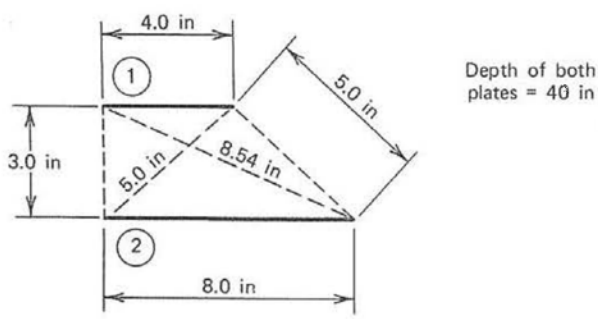

Figure 5.18 End view of two long rectangular parallel plates.

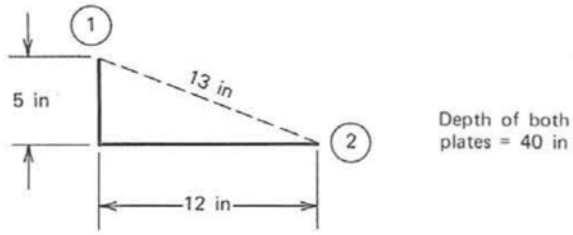

Figure 5.19 End view of two long rectangular perpendicular plates.

The view factor for two long rectangular plates that intersect in a right angle, as shown in Figure 5.19, can be determined with Eq. 5.49. Here the cross strings are the width of each plate, and the noncross string is the hypotenuse of the triangle.

$$A_1 f_{1-2} = A_2 f_{2-1} = \frac{5 + 12 - 13}{2} = 2 \frac{\text{in}^2}{\text{in depth}}$$

The view factor from plates 1 to 2 (f_{1-2}) is

$$f_{1-2} = \frac{A_2 f_{2-1}}{A_1} = \frac{2 \text{ in}^2/\text{in}}{(5)(40) \text{ in}^2}(40 \text{ in}) = 0.40 \text{ (dimensionless)} \qquad (5.52)$$

The view factor from plates 2 to 1 (f_{2-1}) is

$$f_{2-1} = \frac{A_1 f_{1-2}}{A_2} = \frac{2}{(12)(40)} \times 40 = 0.167 \text{ (dimensionless)} \qquad (5.53)$$

Figure 5.20 shows two infinite rectangular parallel plates of width b, directly above one another and separated by a distance h. The view factor

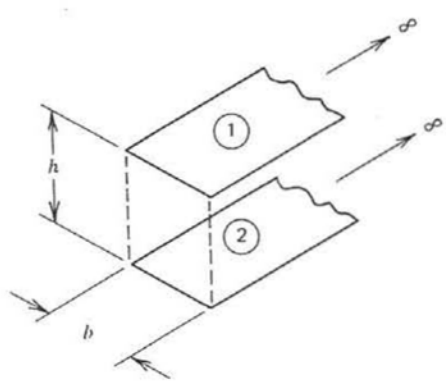

Figure 5.20 Two infinite parallel plates.

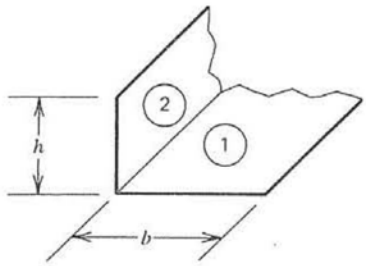

Figure 5.21 Two infinite perpendicular plates.

f_{1-2} is shown by Eq. 5.54.

$$f_{1-2} = \sqrt{1 + \left(\frac{h}{b}\right)^2} - \frac{h}{b} \tag{5.54}$$

When the distance between the plates (h) is equal to the width (b) of the plates, the view factor f_{1-2} is shown by Eq. 5.55.

$$f_{1-2} = \sqrt{1 + (1)^2} - 1 = 1.414 - 1.0 = 0.414 \tag{5.55}$$

Figure 5.21 shows two infinite rectangular plates of width b and h that intersect each other at an angle of 90°. The view factor f_{1-2} is shown by Eq. 5.56.

$$f_{1-2} = \frac{1}{2}\left[1 + \frac{h}{b} - \sqrt{1 + \left(\frac{h}{b}\right)^2}\right] \tag{5.56}$$

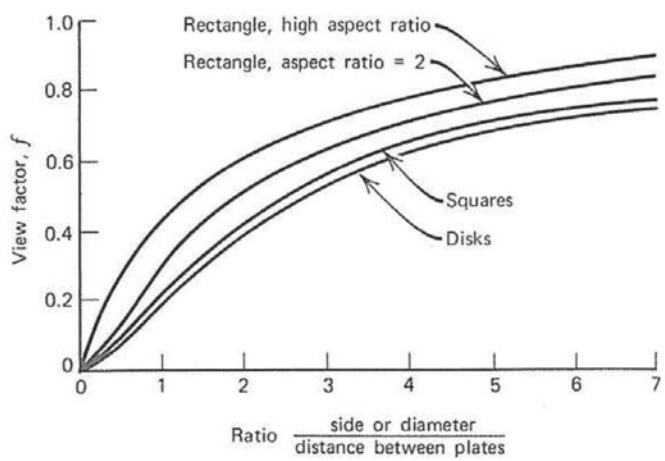

Figure 5.22 View factor for flat parallel plates directly opposed. (From Heat Transmission, by McAdams, McGraw Hill Book Co.)

When the width of both plates are equal, the view factor f_{1-2} is shown by Eq. 5.57.

$$f_{1-2} = \frac{1}{2}[1 + 1 - \sqrt{1 + (1)^2}] = 0.293 \tag{5.57}$$

Figure 5.22 shows view factors for two rectangular parallel plates of equal size but with different ratios of length to width, or aspect ratio [15].

Figure 5.23 shows view factors for two rectangular plates of different sizes that intersect at an angle of 90° [15].

The view factor f is not easily determined for radiation involving irregular shapes, unless the radiating surface (1) is completely enclosed by another surface (2), as shown in Figure 5.24. The view factor from surface 1 to surface 2 (f_{1-2}) is 1.0 for this condition.

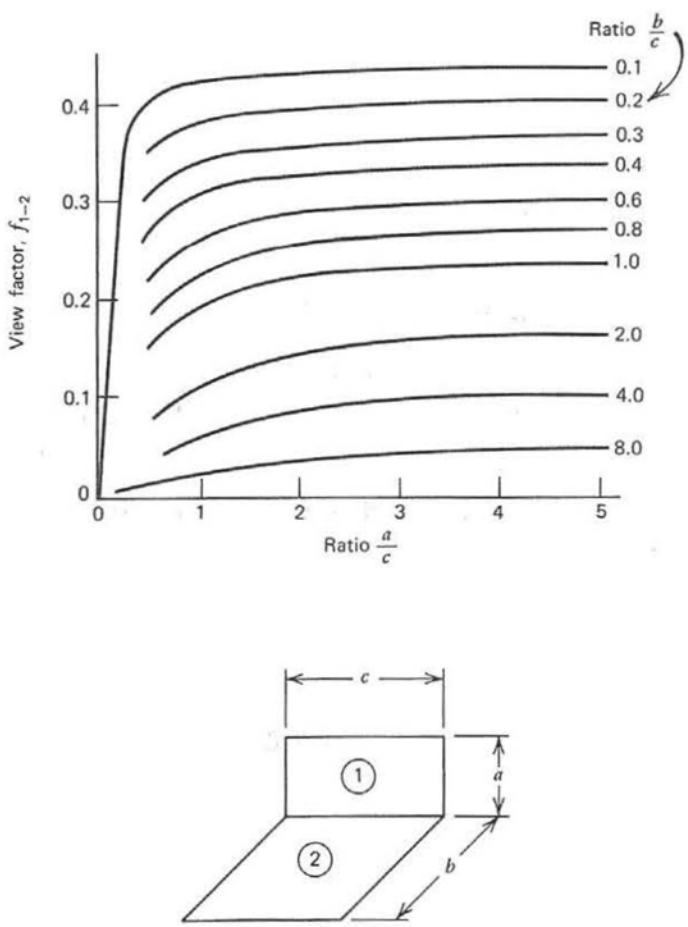

Figure 5.23 View factor for perpendicular and adjacent rectangles with a common side. (From Heat Transmission, by McAdams, McGraw Hill Book Co.)

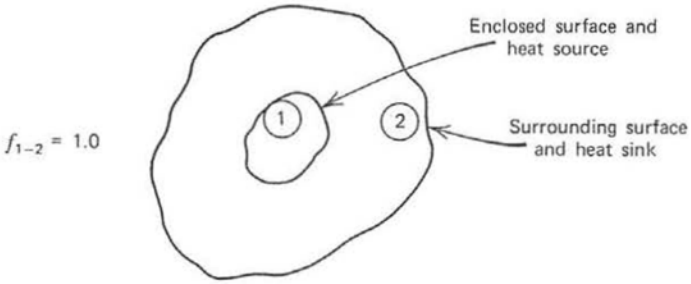

Figure 5.24 View factor for a completely enclosed irregular body.

When partial surfaces are involved in the radiation interchange, the view factor must be calculated or estimated. In electronic systems, the view factor from a transistor on a printed circuit board (PCB) to a cooler wall may be extremely complex and involve lengthy mathematics. If there are 50 transistors in different positions on different PCBs, the calculations may take several weeks. The amount of time required to perform these calculations may not be cost effective, so that the view factors for each transistor may simply be estimated.

Radiation heat transfer depends upon the line of sight. Therefore, it is important to determine approximately what fraction of the radiation leaving the surface of each transistor in all directions is intercepted by the cooler wall. This is what determines the view factor from the transistor to the wall.

The view factor from a hot transistor case on one PCB to the surface of an adjacent PCB is meaningless unless the adjacent PCB is much cooler than the transistor case. In general, there is very little heat lost by radiation between the hot components on adjacent PCBs. These hot components just "see" each other, so that there is a radiation interchange but no heat loss (see Figure 5.25).

Electronic components mounted on the end PCBs will usually have a good view of the end walls. Radiation heat transfer for these components will be relatively good if the end walls are cool.

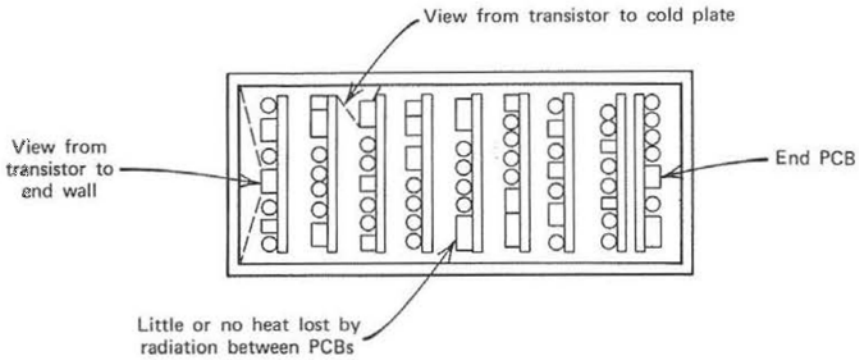

Figure 5.25 Radiation heat transfer within an electronic box.

SEC et al. v. MRI
SEC Exhibit 1027.0156
IPR2023-00255

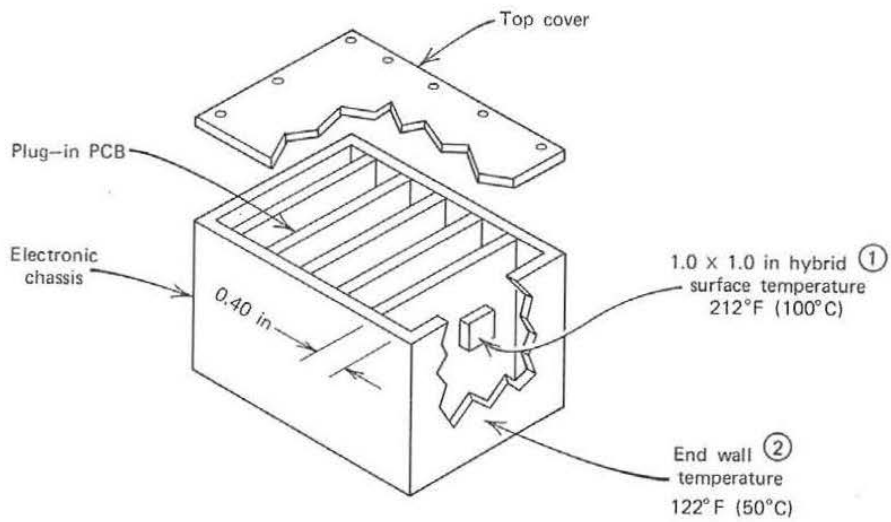

Figure 5.26 Hybrid mounted on a PCB that faces a chassis end wall.

5.18 SAMPLE PROBLEM—RADIATION HEAT TRANSFER FROM A HYBRID

A 1.0 in. square (2.54 cm) × 0.180 in. high (0.457 cm) flat pack hybrid is mounted on the end printed circuit board so that it faces the end wall of an electronic chassis, which has a temperature of 122°F (50°C), as shown in Figure 5.26. The hybrid is about 0.40 in (1.02 cm) from the wall, so that natural convection and conduction heat transfer will be negligible. The maximum allowable case temperature of the hybrid is 212°F (100°C). Determine the maximum allowable power dissipation for the hybrid with and without a conformal coating. The inside surfaces of the aluminum chassis are painted light blue.

SOLUTION

The top surface of the hybrid and its electrical lead wires have a good view of the chassis end wall. The view from the side walls of the hybrid to the side walls of the chassis is blocked by other electronic components around the hybrid. The bottom surface of the hybrid has no view of any wall. Ignoring radiation from the lead wires, the view factor from the top surface of the hybrid to the end wall will be very high, because the end wall is so close to the hybrid and the end wall is so much larger than the hybrid. The view factor f from the hybrid case to the chassis wall in this case would be about 0.95.

SEC et al. v. MRI
SEC Exhibit 1027.0157
IPR2023-00255

Equation 5.47 can be used to determine the amount of heat the hybrid is permitted to dissipate, in English and metric units.

Given $\sigma = 0.1713 \times 10^{-8}$ Btu/hr ft^2 °R^4 = 1.355×10^{-12} cal/sec cm^2 °K^4
$f = 0.95$ estimated, based on geometry
$e_1 = 0.066$ emissivity of bare hybrid steel case
$e_2 = 0.90$ emissivity of painted aluminum wall

$$e = \frac{1}{1/e_1 + 1/e_2 - 1} = \frac{1}{1/0.066 + 1/0.90 - 1} = 0.0655$$

(combined emissivity)

$A_1 = 1.0$ in^2 = 0.00694 ft^2 = 6.45 cm^2 (area)
$t_1 = 212°F = 100°C$ (hybrid case temperature)
$t_2 = 122°F = 50°C$ (chassis wall temperature)

Substitute into Eq. 5.47 for heat transferred from the hybrid by radiation, without a conformal coating, using English units.

$$Q = \left(0.1713 \times 10^{-8} \frac{\text{Btu}}{\text{hr ft}^2\ °\text{R}^4}\right)(0.95)(0.0655)(0.00694\ \text{ft}^2)$$
$$[(460 + 212)^4 - (460 + 122)^4]\ °\text{R}^4$$

$$Q = (0.1713)(0.95)(0.0655)(0.00694)\left[\left(\frac{672}{100}\right)^4 - \left(\frac{582}{100}\right)^4\right]$$

$$Q = 0.065 \frac{\text{Btu}}{\text{hr}} \times 0.293 \frac{\text{watt}}{\text{Btu/hr}} = 0.019 \text{ watt} \tag{5.58}$$

In metric units for the hybrid with no coating:

$$Q = \left(1.355 \times 10^{-12} \frac{\text{cal}}{\text{sec cm}^2\ °\text{K}^4}\right)(0.95)(0.0655)(6.45\ \text{cm}^2)$$
$$[(273 + 100)^4 - (273 + 50)^4]\ °\text{K}^4$$

$$Q = (1.355)(0.95)(0.065)(6.45)\left[\left(\frac{373}{1000}\right)^4 - \left(\frac{323}{1000}\right)^4\right]$$

$$Q = 0.00457 \frac{\text{cal}}{\text{sec}} \times 4.187 \frac{\text{watts sec}}{\text{cal}} = 0.019 \text{ watt} \tag{5.58a}$$

When a thin conformal coating is applied to the hybrid case, the emissivity will jump to about 0.80. The combined emissivity will jump to

$$e = \frac{1}{1/0.80 + 1/0.90 - 1} = 0.734$$

An examination of Eqs. 5.58 and 5.58a shows that the amount of heat transferred by radiation is directly proportional to the emissivity. Therefore,

SEC et al. v. MRI
SEC Exhibit 1027.0158
IPR2023-00255

a direct ratio of the combined emissivities can be used to determine the heat transferred when a conformal coating is added to the hybrid case.

$$Q = 0.019 \text{ watt} \left(\frac{e_{\text{coat}}}{e_{\text{no coat}}}\right) = 0.019 \left(\frac{0.734}{0.0655}\right)$$

$$Q = 0.213 \text{ watt} \tag{5.59}$$

This shows that just adding a conformal coating to the hybrid will increase its heat transfer capability by a factor of 11.

5.19 SAMPLE PROBLEM—JUNCTION TEMPERATURE OF A DUAL FET SWITCH

Figure 5.27 shows a dual field effect transistor (FET) switch in a TO-8 size case that dissipates 0.150 watt. The switch is mounted on a PCB within an electronic chassis that has painted walls at a temperature of 185°F (85°C). The maximum allowable junction temperature is 302°F (150°C) and the thermal impedance (Θ_{jc}) from the junction of the switch to the case is 49.2°F/watt (27.3°C/watt) as rated by the manufacturer. The case of the switch is made of polished iron and the view factor f from the case to the chassis walls is estimated to be about 0.80. The chassis is enclosed, so that natural convection and conduction heat transfer from the switch are negligible. Determine if the design is satisfactory.

SOLUTION

The following information is required for Eq. 5.47.

$f = 0.80$ view factor, estimated from geometry
$e_1 = 0.24$ emissivity of switch with bare iron case
$e_2 = 0.84$ emissivity of painted chassis walls

$$e = \frac{1}{1/e_1 + 1/e_2 - 1} = \frac{1}{1/0.24 + 1/0.84 - 1} = 0.23$$

(combined emissivity)

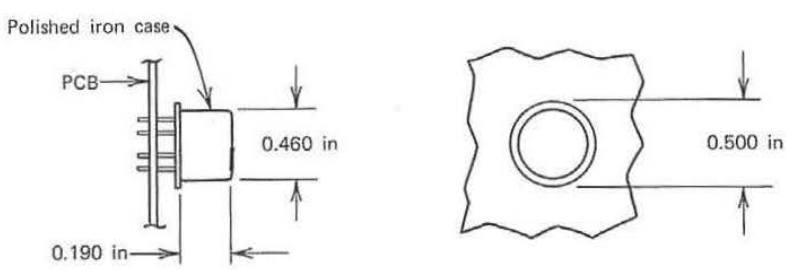

Figure 5.27 Dual FET switch mounted on a PCB.

SEC et al. v. MRI
SEC Exhibit 1027.0159
IPR2023-00255

The bottom surface of the switch faces the PCB, which is a poor heat conductor, so that its area is ignored. Also, radiation from the lead wires is ignored. The switch surface area is:

$$A = \frac{\pi(0.460)(0.190) + (\pi/4)(0.500)^2 \text{ in}^2}{144 \text{ in}^2/\text{ft}^2} = 0.00327 \text{ ft}^2$$

$$Q = 0.150 \text{ watt} \times 3.413 \frac{\text{Btu/hr}}{\text{watt}} = 0.512 \frac{\text{Btu}}{\text{hr}} \text{ (heat dissipation)}$$

Substitute into Eq. 5.47 for the case temperature.

$$0.512 = 0.1713 \times 10^{-8}(0.8)(0.23)(0.00327)[(460 + t_1)^4 - (460 + 185)^4]$$

$$0.512 = 1.031 \times 10^{-12}(460 + t_1)^4 - 0.1784$$

$$460 + t_1 = \left(\frac{0.512 + 0.1784}{1.031 \times 10^{-12}}\right)^{1/4}$$

$$t_1 = 444.6°\text{F } (229.2°\text{C}) \text{ (case temperature)} \tag{5.60}$$

The temperature rise from the switch case to the junction is determined from the manufacturer's thermal impedance from junction to case (Θ_{jc}), 49.2°F/watt.

$$\Delta t_{jc} = 49.2 \frac{°\text{F}}{\text{watt}} \times 0.150 \text{ watt} = 7.4°\text{F} \tag{5.61}$$

The junction temperature becomes

$$t_j = 444.6 + 7.4 = 452°\text{F } (233.3°\text{C}) \tag{5.62}$$

This is substantially above the maximum allowable junction temperature of 302°F (150°C), so that the design is not satisfactory.

To improve the radiation heat transfer, a black oxide finish is added to the surface of the switch, which raises its emissivity to a value of 0.95. The combined emissivity is now

$$e = \frac{1}{1/0.95 + 1/0.84 - 1} = 0.804 \text{ (combined emissivity)}$$

Substitute back into Eq. 5.47 for the case temperature.

$$0.512 = 0.1713 \times 10^{-8}(0.8)(0.804)(0.00327)[(460 + t_1)^4 - (460 + 185)^4]$$

$$460 + t_1 = \left(\frac{0.512 + 0.623}{3.60 \times 10^{-12}}\right)^{1/4}$$

$$t_1 = 289°\text{F } (142.7°\text{C}) \text{ (case temperature)} \tag{5.63}$$

SEC et al. v. MRI
SEC Exhibit 1027.0160
IPR2023-00255

The thermal impedance Θ_{jc} from the junction to the case is still the same. The junction temperature of the switch with the black case is shown as follows:

$$t_j = 289 + 7.4 = 296.4°\text{F } (146.9°\text{C}) \tag{5.64}$$

Since the junction temperature is less than 302°F (150°C), the design is satisfactory.

5.20 RADIATION HEAT TRANSFER IN SPACE

In the hard vacuum environment of space, the amount of radient energy that a body receives will depend upon its distance from the sun, the view the body has of the sun, and its proximity to other planets or satellites. A spacecraft in close orbit around the earth or around the moon can receive radiation from the sun, the earth, and the moon at the same time. Most of this radiation is in the ultraviolet and visible light frequency range, which has a wavelength up to about 1 μm, which is 1×10^{-6} m, as shown in Figure 5.15. In a near earth orbit the direct radiation intensity is about 444 Btu/hr ft^2 (130 watts/ft^2) (0.0334 cal/sec cm^2) [4, 5].

In addition to the direct solar radiation energy, there is reflected radiation energy, or albedo. Albedo is defined as the fraction of solar radiation that is returned to space due to reflections of solar energy from the atmosphere, clouds, and surface of a planet. For the earth, the albedo is about 0.40, depending upon the amount of cloud cover in the sky. For the moon, the albedo is very low, about 0.07, because the moon has virtually no atmosphere.

When the earth is viewed from a distance, its average temperature appears to be about −20°F (−29°C). The mean surface temperature appears to have a value of about 57°F (14°C), and the mean temperature of the upper atmosphere, at about 150,000 ft, is about −85°F (−65°C). The sun, when viewed from a distance, appears to have a temperature of about 10,400°F (5760°C).

The amount of radiant energy that a body in space will receive will depend upon the proximity and the view the body has of the sun and, or the moon, or perhaps some other planet. Table 5.7 shows how much radiant energy various planets receive from the sun. This is the energy that reaches the planet's upper atmosphere, not the energy that reaches the surface (except for the moon).

The upper atmosphere of the earth attenuates the radiation energy received from the sun, and this reduces the amount of solar radiation that actually reaches the surface of the earth. The amount of radiation energy that actually reaches the surface of the earth depends upon the month, hour, parallel of latitude, and cloud cover. Some typical maximum values

SEC et al. v. MRI
SEC Exhibit 1027.0161
IPR2023-00255

Table 5.7 Average Radiation Characteristics of the Planets

Planet	Incident Radiation Intensity (Btu/hr ft²)	Reflected Radiation (Albedo)	Equivalent Black Body Temperature (°F)	
Mercury	2922	0.06	342	
Venus	860	0.61	127	
Earth	444	0.40	−5	Night sky = −40°F
(Moon)	434	0.072	51	
Mars	192	0.15	−56	
Jupiter	16.4	0.41	−242	
Saturn	4.9	0.42	−297	
Uranus	1.2	0.45	−346	
Neptune	0.5	0.54	−366	
Pluto	0.3	0.15	−380	

on a clear day are as follows: [37, 38]:

40° north latitude USA: 300 Btu/hr ft²

32° north latitude USA: 310 Btu/hr ft²

24° north latitude USA: 320 Btu/hr ft²

Deep space has the ability to absorb virtually an infinite amount of heat that makes it a very useful heat sink with a temperature of −460°F (−273°C), absolute zero. The view factor of a body in deep space is 1.0, because the body can radiate to deep space in all directions.

If two aluminum spheres are placed in deep space and if one sphere has a polished aluminum surface while the other sphere has a surface that is painted white, the white sphere will show a steady state surface temperature of about 80°F (26.6°C) and the polished sphere will show a surface temperature of about 450°F (232°C), as shown in Figure 5.28.

5.21 EFFECTS OF α/e ON TEMPERATURES IN SPACE

When thermal radiation energy strikes a body, the fraction of the incident radiation energy that is absorbed is called the absorptivity α. In the infrared, or long wavelength range, the color has no effect on the absorptivity, and a black surface will absorb about the same amount of thermal radiation energy as a white surface. In the visible, or short wavelength range (see Figure 5.15), the amount of radiation energy absorbed by a body is sharply

SEC et al. v. MRI
SEC Exhibit 1027.0162
IPR2023-00255

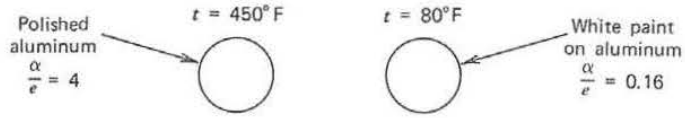

Figure 5.28 Temperatures of painted and unpainted aluminum spheres in space.

affected by its color. The stabilized temperature a body reaches in space will therefore be related to the ratio of the solar absorptivity (α_s) to the infrared emissivity (e), which is shown as the ratio α_s/e. For the polished aluminum sphere this ratio is shown in Eq. 5.65 and for the white-painted aluminum sphere, this ratio is shown in Eq. 5.66.

Polished aluminum sphere in space:

$$\frac{\alpha_s}{e} = \frac{\text{solar absorptivity}}{\text{infrared emissivity}} = \frac{0.10}{0.025} = 4 \tag{5.65}$$

White-painted aluminum sphere in space:

$$\frac{\alpha_s}{e} = \frac{\text{solar absorptivity}}{\text{infrared emissivity}} = \frac{0.15}{0.94} = 0.16 \tag{5.66}$$

A high ratio of α/e means that more solar radiation energy will be absorbed, so that the resulting temperature of a body in space will be higher. Conversely, a low α/e means that less solar radiation energy will be absorbed, so that the resulting temperature will be lower. The equilibrium temperature of a body in space can be controlled, to a great extent, by controlling the ratio of α_s/e.

A body in space will receive radiation from the sun and emit radiation to space at −460°F, which is absolute zero. If the amount of solar energy absorbed by a body (including albedo) is shown as $\alpha_s Q_s A_s$, the general radiation relation shown by Eq. 5.47 can be modified as shown by Eq. 5.67.

$$Q_i + \alpha_s Q_s A_s = \sigma e A T^4 \tag{5.67}$$

where α_s = absorptivity of surface receiving solar radiation
Q_s = solar irradiation on absorbing surface
Q_i = internal power dissipation
A_s = projected area of body normal to sun
σ = Stefan–Boltzmann constant
e = emissivity of surface radiating to space
A = surface area of body radiating to space
T = absolute temperature of body in space

When the body in space is away from all the planets, with no internal power

dissipation and no heat transferred into or out of the back side of the body, and when the projected area of the body is normal to the sun. The absolute temperature of the body in space is shown by Eq. 5.68.

$$T = \left(\frac{\alpha_s Q_s}{\sigma e}\right)^{0.25} \tag{5.68}$$

In a deep space orbit similar to that of Venus, but away from all planets, the direct solar radiation intensity Q_s is about 860 Btu/hr ft^2 (252 watts) (0.0648 cal/sec cm^2). Substitute this value into Eq. 5.68 to obtain the relation for the absolute temperature of a body in a deep space orbit similar to that of Venus.

$$T = \left(\frac{860\alpha_s}{0.1713 \times 10^{-8} e}\right)^{0.25} = 842\left(\frac{\alpha_s}{e}\right)^{0.25} \tag{5.69}$$

Since the solar absorptivity (α_s) and the infrared emissivity (e) are both characteristics of the body surface, the control of these values will help to control the body temperature.

5.22 SAMPLE PROBLEM—TEMPERATURES OF AN ELECTRONIC BOX IN SPACE

An electronic box has an insulated panel with a surface area of 1.0 ft^2. It is in deep space approximately the same distance from the sun as the earth. The panel is painted white and always faces the sun. Determine the stabilized temperature of the panel with no internal power dissipation and with an internal power dissipation of 50 watts.

SOLUTION

Given Q_s = 444 Btu/hr ft^2 solar radiation on panel in an orbit similar to that of Earth
α_s = 0.15 solar absorptivity of white paint (ref. Table 5.4)
σ = 0.1713×10^{-8} Btu/hr ft^2 °R^4 constant
e = 0.9 emissivity of white paint (ref. Table 5.4)

Substitute into Eq. 5.68 for the stabilized temperature of the panel with no internal power dissipation.

$$T = \left[\frac{(0.15)(444)}{(0.1713 \times 10^{-8})(0.9)}\right]^{0.25} = 455.9°\text{R}$$

$$t = 455.9 - 460 = -4.1°\text{F} \tag{5.70}$$

SEC et al. v. MRI
SEC Exhibit 1027.0164
IPR2023-00255

The stabilized temperature of the panel with power on can be obtained with Eqs. 5.67 and 5.68, which requires adding the internal power of 50 watts (170.6 Btu/hr).

$$T = \left[\frac{(0.15)(444) + 170.6}{(0.1713 \times 10^{-8})(0.9)}\right]^{0.25} = 626.3°\text{R}$$

$$t = 626.3 - 460 = 166.3°\text{F} \tag{5.71}$$

If the electronic box was in an orbit around the earth, where it was possible for the panel to receive reflected albedo radiation (40%) from the earth, the panel would receive an additional incident radiation of 444 × 0.40 or 177.6 Btu/hr ft. Substituting into Eq. 5.68 for the panel temperature, we obtain

$$T = \left[\frac{(0.15)(444 + 177.6) + 170.6}{(0.1713 \times 10^{-8})(0.9)}\right]^{0.25} = 643.2°\text{R}$$

$$t = 643.2 - 460 = 183°\text{F} \tag{5.72}$$

There would also be an interchange of radiation energy between the electronic box and the earth, which would depend upon the orbit of the electronic box around the planet. This energy interchange was ignored in the problem.

5.23 SIMPLIFIED RADIATION HEAT TRANSFER EQUATION

It is often convenient to express the radiation heat loss in a form similar to the convection heat loss, as shown by Eq. 5.7. This can be accomplished by setting Eq. 5.7 equal to Eq. 5.47. The radiation heat transfer equation is then simplified as shown by Eq. (5.73) [15, 17, 24].

$$Q = h_r A \, \Delta t \tag{5.73}$$

In this expression, h_r represents the radiation heat transfer coefficient in terms of Btu/hr ft² °F (cal/sec cm² °C). The radiation coefficient is then defined as shown in Eq. 5.74 for English units and in Eq. 5.74a for metric units.

$$h_r = \frac{0.1713 fe \{[(t_1 + 460)/100]^4 - [(t_2 + 460)/100]^4\}}{t_1 - t_2}$$

$$= \frac{\text{Btu}}{\text{hr ft}^2\ °\text{F}} \tag{5.74}$$

SEC et al. v. MRI
SEC Exhibit 1027.0165
IPR2023-00255

$$h_r = \frac{1.355 fe \{[(t_1 + 273)/1000]^4 - [(t_2 + 273)/1000]^4\}}{t_1 - t_2}$$

$$= \frac{\text{cal}}{\text{sec cm}^2\,°\text{C}} \tag{5.74a}$$

A plot of Eq. 5.74 is shown in Figure 5.29 for various heat receiver temperatures and various temperature differences between the emitting and receiving surfaces [70].

5.24 SAMPLE PROBLEM—RADIATION HEAT LOSS FROM AN ELECTRONIC BOX

An electronic box, for a space application, has hybrid circuits mounted on the cover facing the inside of the box. The backside of the cover can "see" the back side of a space radiator panel within the spacecraft, as shown in Figure 5.30. The maximum allowable hybrid case temperature is 212°F (100°C). The temperature rise from the component case to the cover is 12°F (6.7°C), which means that the maximum allowable cover temperature is 200°F (93.3°C). The radiator panel has a temperature of 20°F (−6.7°C) and an emissivity e_2 of 0.75. The electronic box cover has a painted finish with an emissivity e_1 of 0.85. Determine the maximum allowable power the electronic components on the cover can dissipate.

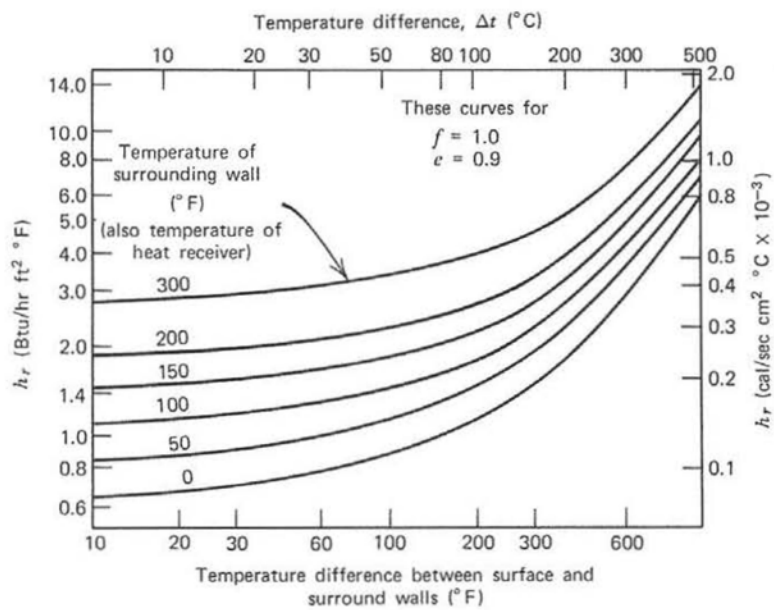

Figure 5.29 Radiation heat transfer as a function of temperature. (From General Electric Co. Heat Transfer/Fluid Flow Data Book)

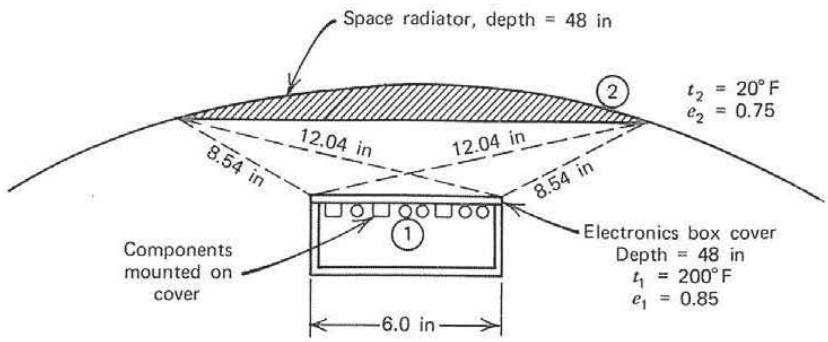

Figure 5.30 Electronic box mounted in a spacecraft.

SOLUTION

The cross string method shown in Eq. 5.49 is used to determine the view factors between the radiating surfaces.

$$A_1 f_{1-2} = A_2 f_{2-1} = \frac{2(12.04) - 2(8.54)}{2} = 3.5 \frac{\text{in}^2}{\text{in depth}}$$

$$f_{1-2} = \frac{A_2 f_{2-1}}{A_1} = \frac{3.5 \text{ in}^2/\text{in}}{(6)(48) \text{ in}^2} \times 48 \text{ in} = 0.583$$

$$f_{2-1} = \frac{A_1 f_{1-2}}{A_2} = \frac{3.5}{(12)(48)} \times 48 \text{ in} = 0.292$$

The combined emissivity is obtained from Table 5.5.

$$e = \frac{1}{1/e_1 + 1/e_2 - 1} = \frac{1}{1/0.85 + 1/0.75 - 1} = 0.662$$

The view factor from area 1 to area 2 ($f_{1-2} = 0.583$) will be used for the radiation heat transfer, so area 1 must be computed.

$$A_1 = \frac{(6)(48) \text{ in}^2}{144 \text{ in}^2/\text{ft}^2} = 2.0 \text{ ft}^2 = 1858 \text{ cm}^2 \tag{5.75}$$

Substitute into Eq. 5.74 to obtain the radiation coefficient in English Units.

$$h_r = \frac{0.1713(0.583)(0.662)\{[(200 + 460)/100]^4 - [(20 + 460)/100]^4\}}{200 - 20}$$

$$h_r = 0.502 \frac{\text{Btu}}{\text{hr ft}^2\ ^\circ\text{F}} \tag{5.76}$$

SEC et al. v. MRI
SEC Exhibit 1027.0167
IPR2023-00255

Substitute into Eq. 5.74a to obtain the radiation coefficient in metric units.

$$h_r = \frac{1.355(0.583)(0.662)\{[(93.33 + 273)/1000]^4 - [(-6.7 + 273)/1000]^4\}}{93.3 - (-6.7)}$$

$$h_r = 0.0000679 \frac{\text{cal}}{\text{sec cm}^2\ ^\circ\text{C}} \tag{5.76a}$$

Substitute Eqs. 5.75 and 5.76 into Eq. 5.73 for the maximum heat that can be transferred by radiation, using English units.

$$Q = \left(0.502 \frac{\text{Btu}}{\text{hr ft}^2\ ^\circ\text{F}}\right)(2.0\ \text{ft}^2)(200 - 20)^\circ\text{F}$$

$$Q = 180.7 \frac{\text{Btu}}{\text{hr}} \times 0.293 \frac{\text{watt}}{\text{Btu/hr}} = 52.9\ \text{watts} \tag{5.77}$$

Substitute into Eq. 5.73 for the maximum heat that can be transferred by radiation using metric units.

$$Q = \left(0.0000679 \frac{\text{cal}}{\text{sec cm}^2\ ^\circ\text{C}}\right)(1858\ \text{cm}^2)[(93.3 - (-6.7)]$$

$$Q = 12.61 \frac{\text{cal}}{\text{sec}} \times 4.187 \frac{\text{watts}}{\text{cal/sec}} = 52.8\ \text{watts} \tag{5.77a}$$

The heat transfer coefficient h_r could also have been obtained from Figure 5.29 for English units and metric units. Notice that Figure 5.29 is based upon a view factor of 1 and a combined emissivity of 0.9. If the geometry under consideration has a different view factor and a different emissivity, corrections must be applied to obtain the true radiation coefficient.

For the previous problem, using a heat sink temperature of 20°F and a ΔT of 200 − 20 = 180°F, h_r = 1.18 Btu/hr ft² °F for English units. Corrections must be applied for view factors and emissivity.

$$h_r = 1.18 \times 0.583 \times \left(\frac{0.662}{0.9}\right) = 0.506 \frac{\text{Btu}}{\text{hr ft}^2\ ^\circ\text{F}} \tag{5.78}$$

Equation 5.78 compares well with Eq. 5.76.

5.25 COMBINING CONVECTION AND RADIATION HEAT TRANSFER

In many electronic boxes, radiation heat transfer and convection (both natural and forced) occur simultaneously. Therefore, it is convenient to write the combined heat transfer equation in a form similar to the general

SEC et al. v. MRI
SEC Exhibit 1027.0168
IPR2023-00255

relation shown by Eqs. 5.7 and 5.73. The combined relation is shown in Eq. 5.79 [15, 17, 24].

$$Q = (h_c + h_r)A\,\Delta t \tag{5.79}$$

where h_c = Btu/hr ft² °F or cal/sec cm² °C (convection coefficient)
h_r = Btu/hr ft² °F or cal/sec cm² °C (radiation coefficient)
A = ft² or cm² (area)
Δt = °F or °C (temperature difference, surface to ambient)

For most small electronic boxes, typical values of h_c are about 0.8 Btu/hr ft² °F (0.000108 cal/sec cm² °C) and typical values of h_r are about 1.2 Btu/hr ft² °F (0.000162 cal/sec cm² °C), which results in a combined heat transfer coefficient, $h_c + h_r$, of about 2.0 Btu/hr ft² °F (0.00027 cal/sec cm² °C).

5.26 SAMPLE PROBLEM—ELECTRONIC BOX IN AN AIRPLANE COCKPIT AREA

An electronic box is mounted in the cockpit area of an airplane that must operate at 50,000 ft without a pressurized cabin. Plug-in PCBs within the box are cooled by conducting their heat to the side walls of the electronic box. Natural convection and radiation are used to cool the external surfaces of the box. The maximum expected cockpit temperature is 100°F and the maximum allowable box surface temperature is 140°F. Because the top and bottom covers are fastened to the box with a few small screws, the covers make poor contact with the box and will not be effective heat transfer surfaces (see Figure 5.31). Determine the maximum amount of heat that can

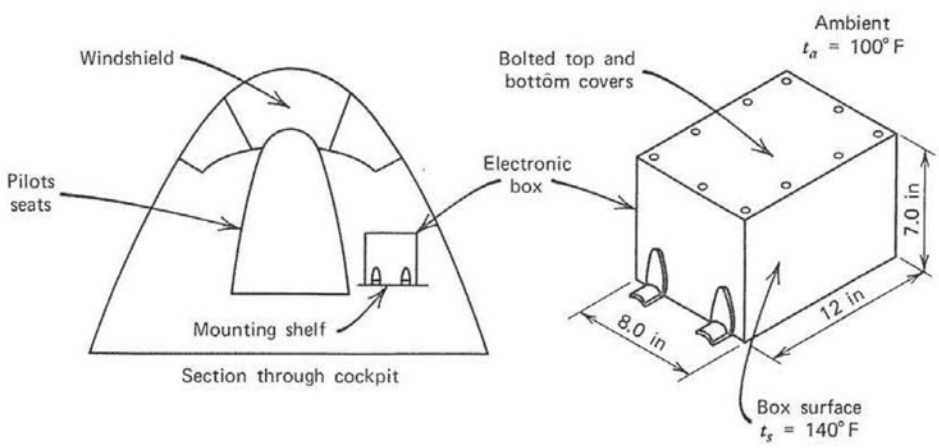

Figure 5.31 Electronic box mounted on a shelf in an airplane.

SEC et al. v. MRI
SEC Exhibit 1027.0169
IPR2023-00255

be transferred from the box to the surrounding ambient at sea level and at 50,000 ft. The box has painted external surfaces.

SOLUTION

Only the vertical side and end walls will be effective for heat transfer by natural convection and radiation. The top and bottom covers are ignored here because the covers make poor contact with the chassis. The natural convection coefficient for the vertical side and end walls is determined first for the sea level condition.

$$h_c = 0.29\left(\frac{\Delta t}{L}\right)^{0.25} \qquad \text{(ref. Eq. 5.4)}$$

Given $\Delta t = 140 - 100 = 40°\text{F}$ (temperature difference)

$$L = \frac{7.0\text{ in}}{12\text{ in/ft}} = 0.583\text{ ft (vertical height)}$$

$$h_c = 0.29\left(\frac{40}{0.583}\right)^{0.25} = 0.83\,\frac{\text{Btu}}{\text{hr ft}^2\,°\text{F}}\text{ (convection coefficient)} \qquad (5.80)$$

The radiation heat transfer coefficient is determined next, using an emissivity of 0.9 for the painted finish and a view factor of 1.0 for the electronic box. Using Figure 5.29 with an ambient heat sink temperature of 100°F and a Δt of 40°F,

$$h_r = 1.20\,\frac{\text{Btu}}{\text{hr ft}^2\,°\text{F}}\text{ (radiation coefficient)} \qquad (5.81)$$

The surface area available for heat transfer is the sides and ends of the box only.

$$A = \frac{(2 \times 12 + 2 \times 8)(7)\text{ in}^2}{144\text{ in}^2/\text{ft}^2} = 1.94\text{ ft}^2 \qquad (5.82)$$

Substitute Eqs. 5.80 through 5.82 into Eq. 5.79 for the heat transferred at sea level conditions.

$$Q = (0.83 + 1.20)(1.94)(40)$$

$$Q = 157.5\,\frac{\text{Btu}}{\text{hr}} \times 0.293\,\frac{\text{watt}}{\text{Btu/hr}} = 46.1\text{ watts} \qquad (5.83)$$

At an altitude of 50,000 ft, there will be a small change in the radiation characteristics of the box, but there will be a big change in the natural

SEC et al. v. MRI
SEC Exhibit 1027.0170
IPR2023-00255

convection characteristics. (The surface temperature of the box will increase slightly at altitude.)

$$h_{\text{alt}} = h_c \sqrt{\frac{\text{altitude pressure}}{14.7 \text{ psia}}} \text{ (ref. Eq. 5.41)}$$

Using the pressure altitude from Table 6.5, the pressure at 50,000 ft is 1.692 lb/in^2.

$$h_{\text{alt}} = 0.83 \sqrt{\frac{1.69 \text{ psia}}{14.7 \text{ psia}}} = 0.28 \frac{\text{Btu}}{\text{hr ft}^2\ ^\circ\text{F}} \tag{5.84}$$

Equation 5.79 is used once again to determine the amount of heat that can be transferred at the 50,000 ft altitude.

$$Q = (h_{\text{alt}} + h_r)\dot{A}\ \Delta T \qquad \text{(ref. Eq. 5.79)}$$

$$Q = (0.28 + 1.20)(1.94)(40)$$

$$Q = 114.8 \frac{\text{Btu}}{\text{hr}} \times 0.293 \frac{\text{watt}}{\text{Btu/hr}} = 33.6 \text{ watts} \tag{5.85}$$

This shows that the amount of heat that can be removed at the 50,000 ft altitude has been reduced about 27%.

5.27 EQUIVALENT AMBIENT TEMPERATURE FOR RELIABILITY PREDICTIONS

Reliability failure rates for electronic component parts are usually shown to be related to the *ambient* temperature in which the component is operating. MIL-HDBK-217B, for example, shows failure rates for various components as a function of the ambient temperature [39].

In many electronic systems, the electronic components are mounted on thermally conductive circuit boards, which spread the heat to eliminate hot spots and also carry the heat to cold plates and heat exchangers. A low thermal resistance path is provided from the component surface directly to the chassis heat sink. This technique is very effective in providing a low component *surface* temperature.

The reliability engineer is not interested in component surface temperatures, because there are very few data relating surface temperatures of components to failure rates. Most data will show that component failure rates are related to the ambient temperature. Therefore, reliability engineers will usually request information relating to ambient temperatures when they are computing failure rates for a system.

SEC et al. v. MRI
SEC Exhibit 1027.0171
IPR2023-00255

When components are cooled by conduction, there are no real ambient operating temperatures that can be used to predict failure rates. However, an equivalent ambient temperature can be calculated based upon the surface temperature of the component. Thus, for a given set of conditions and for specific components, the equivalent ambient temperature can be determined from the component surface temperature. This permits failure rates to be determined for components when only the surface temperatures are known.

Since heat travels from high temperature areas to low temperature areas, it follows that a heat dissipating component will be hotter than the ambient temperature surrounding the component.

When an electronic component is suspended in a controlled environmental chamber, heat is transferred from the component to the surrounding ambient by means of radiation and natural convection. Component manufacturers and component testing engineers often use this technique to determine how much power a component can dissipate and what the failure rates are for various ambient temperature conditions.

The surface temperature of a component on a PCB is usually known from test data, or it can be calculated. The equivalent ambient temperature for the same component (the ambient temperature that will result in the same component surface temperature) is determined by obtaining the temperature rise from the component to the surrounding ambient using Eq. 5.86.

$$t_s = t_a + \Delta t_{s-A} \tag{5.86}$$

where t_s = component surface temperature
t_a = ambient temperature
Δt_{s-A} = temperature rise from surface to ambient

The temperature rise from the component surface to the ambient Δt_{s-A} is determined from Eq. 5.79.

$$\Delta t_{s-A} = \frac{Q}{(h_c + h_r)A} \qquad \text{(ref. Eq. 5.79)}$$

The physical properties of the component are used to determine the surface area, the radiation coefficient, and the natural convection coefficient. The electrical lead wires are ignored in these calculations because they are usually very short in most applications, so that they will transfer very little heat by radiation and natural convection.

Radiation depends upon the actual surface temperature of the component, which is unknown. Therefore, the method of solution is to assume a temperature rise (Δt) that permits the radiation and natural convection coefficients to be determined. A Δt value is then calculated from the coefficients and compared with the assumed value. If the Δt's do not agree, a correction is made and the process is repeated until the assumed Δt agrees relatively

SEC et al. v. MRI
SEC Exhibit 1027.0172
IPR2023-00255

well with the calculated Δt. A sample problem is used to demonstrate the technique.

5.28 SAMPLE PROBLEM—EQUIVALENT AMBIENT TEMPERATURE OF AN RC07 RESISTOR

A MIL style RC07 $\frac{1}{4}$ watt carbon composition resistor, as shown in Figure 5.32, dissipates 0.125 watt when it is mounted on a PCB that is cooled by conduction. A small thermocouple on the resistor shows that the surface temperature is 212°F (100°C) in the operating environment. The reliability engineer must determine the mean time between failures (MTBF) for this resistor. The only failure rate data are based on ambient temperatures. Determine the equivalent *ambient* temperature that will produce the same failure rate as a component *surface* temperature of 212°F (100°C).

SOLUTION

The lead wires are small compared to the body of the resistor, so that they are ignored. Assume that the resistor body is suspended in a temperature-controlled chamber. The natural convection coefficient can then be determined from Eq. 5.3 and Table 5.1, using a C value of 1.39 for small components in free air.

$$h_c = 0.52C\left(\frac{\Delta t}{L}\right)^{0.25} \qquad \text{(ref. Eq. 5.3)}$$

$$h_c = 0.52(1.39)\left(\frac{\Delta t}{L}\right)^{0.25} = 0.72\left(\frac{\Delta t}{L}\right)^{0.25} \tag{5.87}$$

Since the Δt is not known yet, assume a value of 67°F to start, and calculate the natural convection coefficient from Eq. 5.87.

Given $\Delta t = 67°\text{F}$ (assumed to start)

$$L = \frac{0.098 \text{ in}}{12 \text{ in/ft}} = 0.0082 \text{ ft diameter}$$

$$h_c = 0.72\left(\frac{67}{0.0082}\right)^{0.25} = 6.84\,\frac{\text{Btu}}{\text{hr ft}^2\ °\text{F}} \tag{5.88}$$

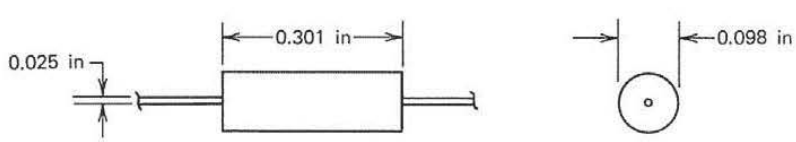

Figure 5.32 MIL style RC 07 carbon composition $\frac{1}{4}$ watt resistor.

SEC et al. v. MRI
SEC Exhibit 1027.0173
IPR2023-00255

The radiation coefficient h_r is determined from Figure 5.29, which is based upon an emissivity of 0.9 and a view factor of 1.0. The view factor of the resistor in the chamber will be 1.0 and the emissivity e of the resistor surface is about 0.9, so that the curves in Figure 5.29 can be used directly with no correction factors. The temperature of the surrounding walls is the same as the ambient temperature t_a, which is determined from Eq. 5.86.

Given $t_s = 212°\text{F}$ (surface temperature)
$\Delta t_{s-A} = 67°\text{F}$ (assumed to start)
$t_a = t_s - \Delta t_{s-A} = 212 - 67 = 145°\text{F}$ (ambient)

From Figure 5.29:

$$h_r = 1.61 \frac{\text{Btu}}{\text{hr ft}^2\ °\text{F}} \tag{5.89}$$

Also,

$$Q = 0.125 \text{ watts} \times \frac{3.413 \text{ Btu/hr}}{\text{watt}} = 0.427 \frac{\text{Btu}}{\text{hr}} \text{ (heat)}$$

$$A = \frac{(2)(\pi/4)(0.098)^2 + \pi(0.098)(0.301) \text{ in}^2}{144 \text{ in}^2/\text{ft}^2} = 0.000748 \text{ ft}^2 \text{ (area)}$$

Substitute into Eq. 5.79 and solve for Δt.

$$\Delta t = \frac{Q}{(h_c + h_r)\,A} = \frac{0.427}{(6.84 + 1.61)(0.000748)} = 67.5°\text{F} \tag{5.90}$$

Since the calculated Δt of 67.5°F is close to the assumed value of 67°F, the assumed Δt is valid.

The equivalent ambient temperature that can be used for reliability predictions is determined from Eq. 5.86.

$$t_a = t_s - \Delta t_{s-A} = 212 - 67 = 145°\text{F} \tag{5.91}$$

This means that the RC07 resistor will have a surface temperature of 212°F in an ambient temperature of 145°F when the resistor dissipates 0.125 watt. Reliability failure rate predictions will be based upon operation in a 145°F ambient environment.

5.29 INCREASE IN EFFECTIVE EMITTANCE ON EXTENDED SURFACES

Extended surfaces, such as fins, are often used to improve the heat transfer characteristics of electronic equipment. A substantial improvement is ob-

SEC et al. v. MRI
SEC Exhibit 1027.0174
IPR2023-00255

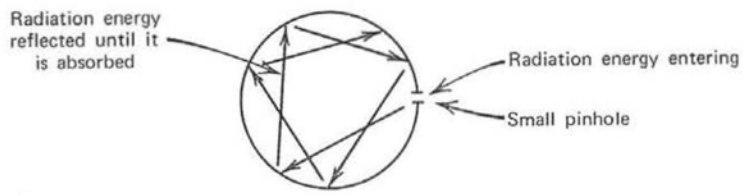

Figure 5.33 Black body represented by a hollow sphere with a pin hole.

tained with convection heat transfer, because the heat removed is directly related to the fin surface area. With radiation, the heat transfer is related to the projected fin area and the emittance of the surface.

A rough surface has a higher emittance than the same surface when it is smooth. Also, a finned surface has a higher emittance than does the same surface without fins. In both cases the emittance increases because the surfaces have many small cavities. These cavities act somewhat like many small partial black bodies [24].

A perfect black body is one that absorbs 100% of all the energy it receives without reflecting any energy. A small hole in a hollow sphere is often used to represent a black body. The energy enters the small opening and strikes the opposite wall, where part of the energy is absorbed and part is reflected. The reflected energy again strikes the opposite wall, where part of the energy is absorbed and again part is reflected. This process continues until all of the energy is absorbed, as shown in Figure 5.33.

Since finned surfaces act somewhat like cavities, a deeper fin should have a higher emittance than a shallow fin. When the emittance of the flat surface is known, the effective emittance of the finned surface can be approximated from Figure 5.34.

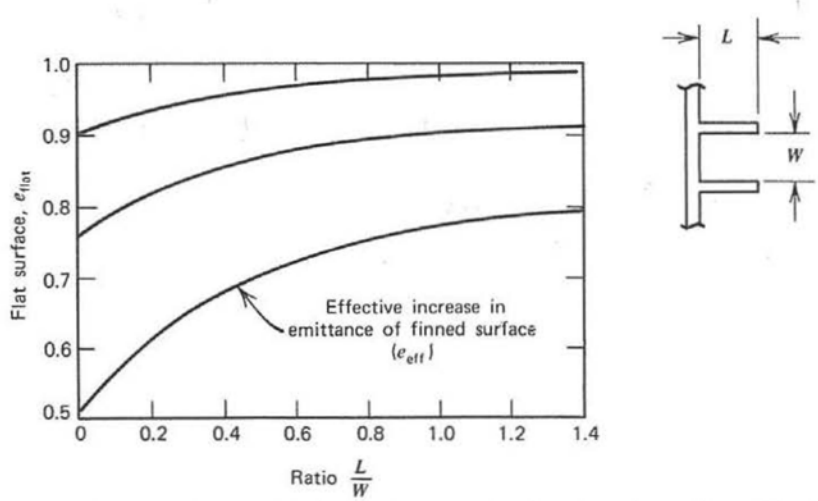

Figure 5.34 Increase in the effective emittance of a finned surface. (From Handbook of Electronic Packaging, by Harper, McGraw Hill Book Co.)

The height of the fin is shown by L and the distance between the fins is shown by W. Dimensions can be in inches or centimeters.

Figure 5.34 shows that the effective emittance of the finned surface can be substantially increased for low emittance surfaces, when the ratio of L/W is greater than 1.0, as shown by Eq. 5.92.

Figure 5.35 Tall single bay cabinet, with a blower at the bottom, for cooling panel and drawer mounted electronics. (Courtesy Litton Systems, Inc.)

SEC et al. v. MRI
SEC Exhibit 1027.0176
IPR2023-00255

$$e_{\text{eff}} = e_{\text{flat}} + \left(\frac{1 - e_{\text{flat}}}{2}\right) \tag{5.92}$$

When e_{flat} is 0.5, then for a L/W ratio of 1.0 the effective emissivity e_{eff} becomes

$$e_{\text{eff}} = 0.5 + \frac{1 - 0.5}{2} = 0.5 + 0.25 = 0.75 \text{ (approximately)}$$

Figure 5.35 shows a tall cabinet that is cooled by means of a blower in the base.

SEC et al. v. MRI
SEC Exhibit 1027.0177
IPR2023-00255

6

Forced Air Cooling for Electronics

6.1 FORCED COOLING METHODS

Heat transfer by forced convection generally makes use of a fan, blower, or pump to provide high velocity fluid (air or liquid) past a heated surface. The high velocity fluid results in a decreased thermal resistance across the boundary layer from the fluid to the heated surface. This, in turn, increases the amount of heat that is carried away by the fluid [40–42].

Forced air systems can provide heat transfer rates in electronic systems that are 10 times greater than those available with natural convection and radiation. Forced liquid cooling systems can provide heat transfer rates that are 10 times greater than those for forced air cooling systems. The penalty for increased cooling is increased costs, power, noise, and complexity. For liquid cooled systems the size and weight may also increase. Since a simple system is generally a more reliable system, heat transfer by natural convection and radiation should be used wherever possible.

The rewards of forced convection cooling techniques are generally reduced size for air cooled systems and higher component densities, with lower hot spot temperatures. This increases the electronic component reliability but requires added maintenance for the extra fans or pumps.

A liquid cooled system is usually larger and heavier than an air cooled system, because a reservoir is generally required for the liquid. A fan cooled system, on the other hand, normally has a large supply of air readily available with no storage requirements, which reduces the size and weight of the system.

Laminar flow conditions as well as turbulent flow conditions can exist with forced convection in liquids and air. Turbulent flow conditions are much more desirable, because they permit more heat to be removed. However, turbulent flow will usually result in a higher pressure drop through the system, which requires that larger pumps and fans and more power be used to overcome the added resistance.

SEC et al. v. MRI
SEC Exhibit 1027.0178
IPR2023-00255

6.2 COOLING AIR FLOW DIRECTION FOR FANS

When a fan is used for cooling electronic equipment, the air flow direction can be quite important. The fan can be used to draw air through a box or to blow air through a box. A blowing fan system will raise the internal air pressure within the box, which will help to keep dust and dirt out of a box that is not well sealed. A blowing system will also produce slightly more turbulence, which will improve the heat transfer characteristics within the box. However, when an axial flow fan is used in a blowing system, the air may be forced to pass over the hot fan motor, which will tend to heat the air as it enters the electronic box, as shown in Figure 6.1.

An exhaust fan system, which draws air through an electronic box, will reduce the internal air pressure within the box. If the box is located in a dusty or dirty area, the dust and dirt will be pulled into the box through all of the small air gaps if the box is not sealed. In an exhaust system, the cooling air passes through an axial flow fan as the air exits from the box, as shown in Figure 6.2. The cooling air entering the electronic box is therefore cooler.

The position of the fan blades within an axial flow fan housing can be a critical factor in determining how well a fan will perform. This is especially important in high speed fans that have speeds greater than about 8000 rpm.

An examination of most high speed axial flow fans will show that the fan blades are not located at the center of the tubular housing but near one end. When the fan is located adjacent to a restricted area, such as a 90° bend, the fan blades should be positioned so that they are at the downstream end of the housing, for the best performance. Air has weight and kinetic energy, so that the air velocity must be allowed to develop to effectively overcome the flow resistance. When the fan blades are located at the downstream end of the fan housing, the air has a slightly longer flow path. This improves the velocity profile, as shown in Figures 6.3 and 6.4.

It makes no difference if a blowing or an exhaust fan system is used; the velocity profile must have a chance to develop to provide an efficient air delivery system.

The reduced flow efficiency for the fan shown in Figure 6.4 will not be obvious to a casual observer. When the fan is in operation, you can place your hand over the exhaust and feel a large volume of air flowing through the fan. However, if a thin strip of paper is slowly passed across the fan exhaust, it will show that some of the air is being short-circuited. The air

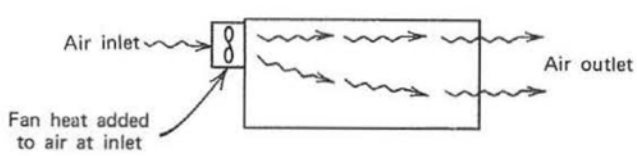

Figure 6.1 Axial flow fan blowing cooling air through a box.

SEC et al. v. MRI
SEC Exhibit 1027.0179
IPR2023-00255

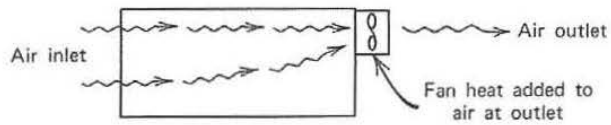

Figure 6.2 Axial flow fan drawing cooling air through a box.

flow at the outer perimeter of the fan will be moving away from the fan, but the air flow at the center will be moving toward the fan, resulting in a short circuit, as shown in Figure 6.5.

Some good fan installations and some poor ones are shown in Figure 6.6. Test data on these types of installations have shown that the cooling air flow rate can be more than doubled just by properly orienting the position of the fan blade within the fan housing when the fan is located adjacent to an area that restricts the free flow of cooling air.

6.3 STATIC PRESSURE AND VELOCITY PRESSURE

Air flow through an electronic box is due to a pressure difference between two points in the box, with the air flowing from the high pressure area to the low pressure area. The flow of air will result in a static pressure and a velocity pressure.

Static pressure is the pressure that is exerted on the walls of the container or electronic box, even when there is no flow of air; it is independent of the air velocity. Static pressure can be positive or negative, depending upon whether it is greater or less than the outside ambient pressure.

Velocity pressure is the pressure that forces the air to move through the electronic box at a certain velocity. The velocity pressure depends upon the velocity of the air and always acts in the direction of the air flow.

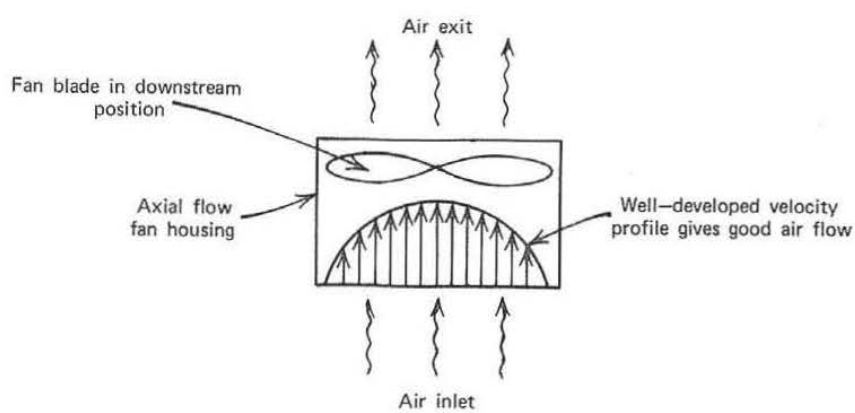

Figure 6.3 Well-developed velocity profile in an axial flow fan.

SEC et al. v. MRI
SEC Exhibit 1027.0180
IPR2023-00255

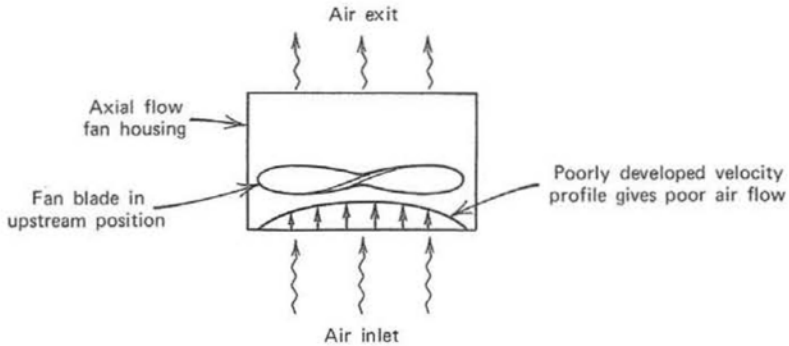

Figure 6.4 Poorly developed velocity profile in an axial flow fan.

The amount of cooling air flowing through an electronic box will usually determine the amount of heat removed from the box. If more air flows through the box, more heat will be removed. As the air flow through the box increases, however, it requires an even greater pressure to force the air through the box.

Static and velocity pressures can be expressed in lb/in^2 and g/cm^2. However, these values are usually very small, so that it is often more convenient to express these pressures in terms of the height of a column of water. For example, 1.0 lb/in^2 (70.37 g/cm^2) equals 27.7 in of water (70.37 cm of water), or 1.0 in of water (2.54 cm of water) equals 0.036 lb/in^2 (2.54 g/cm^2). The water column height is called the "head" of water and is shown as H_s for the static head and as H_v for the velocity head.

The velocity head (H_v) is a convenient reference that is often used to determine pressure drops through electronic boxes. The velocity head can be related to the air flow velocity with the use of Eq. 6.1 [10, 18, 69].

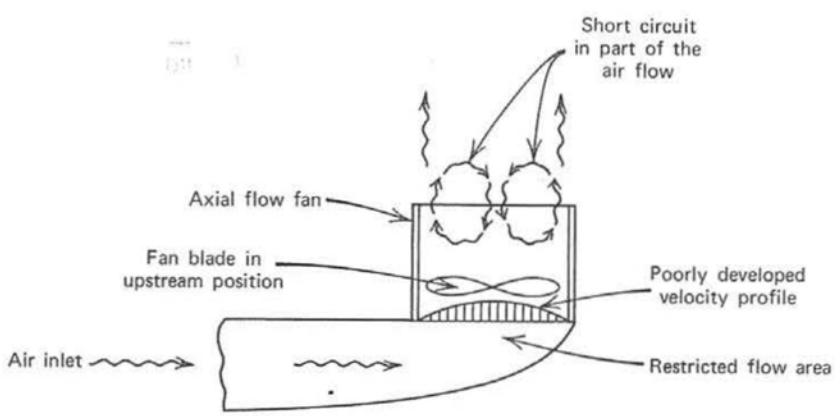

Figure 6.5 Short circuit in part of the cooling air flow due to improper positioning of the fan blades adjacent to a restricted flow area.

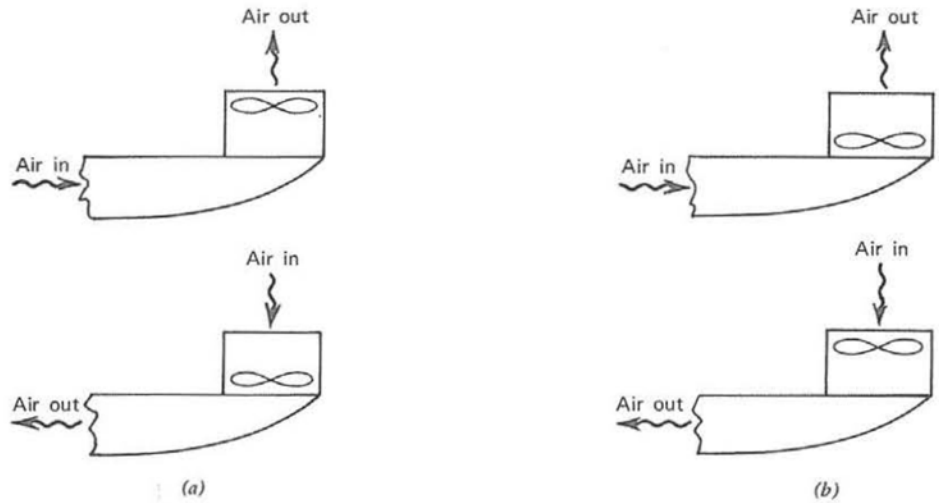

Figure 6.6 Examples of good fan installations and poor fan installations on axial flow fans located adjacent to restricted areas. (*a*) Good fan installations; (*b*) poor fan installations.

$$V = \sqrt{2gH} \tag{6.1}$$

where V = velocity = ft/sec
g = acceleration of gravity = ft/sec^2
H = height = ft

When the air velocity is expressed in feet per minute and the height is expressed as the velocity head H_v in inches of water, Eq. 6.1 can be modified using standard air with a density of 0.0750 lb/ft^3 at 69°F and 14.7 psia. For English units, this is shown in Eq. 6.2.

$$V = 60\,\frac{\text{sec}}{\text{min}}\sqrt{\frac{2(32.14\ \text{ft/sec}^2)(62.4\ \text{lb/ft}^3\ \text{water})(H_v\ \text{in water})}{(12\ \text{in/ft})(0.0750\ \text{lb/ft}^3\ \text{standard air})}}$$

$$V = 4005\sqrt{H_v\,(\text{in water})} = \frac{\text{ft}}{\text{min}} \tag{6.2}$$

For metric units, this is shown in Eq. 6.2a.

$$V = \sqrt{\frac{2(979.6\ \text{cm/sec}^2)(1\ \text{g/cm}^3\ \text{water})(H_v\ \text{cm water})}{0.0012\ \text{g/cm}^3\ \text{air at } 20.5°\text{C}}}$$

$$V = 1277\sqrt{H_v\,(\text{cm water})} = \frac{\text{cm}}{\text{sec}} \tag{6.2a}$$

A sealed electronic box with a gauge pressure of 0.05 lb/in^2 (3.518 g/cm^2)

SEC et al. v. MRI
SEC Exhibit 1027.0182
IPR2023-00255

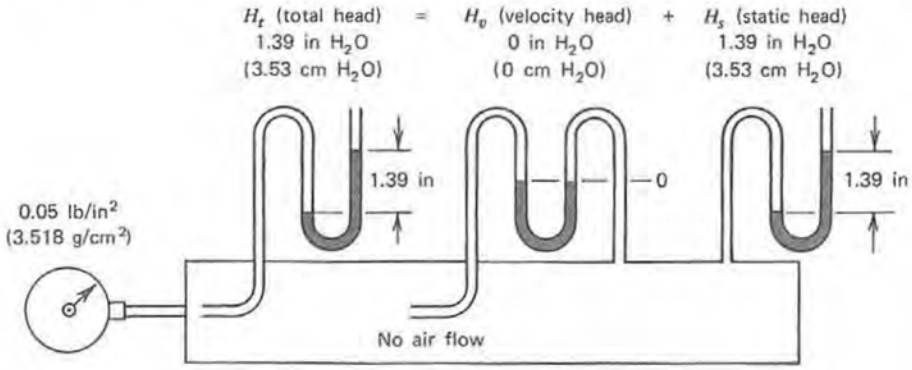

Figure 6.7 A pressurized electronic box with no air flow.

with no air flow will have a pressure equal to the static pressure. If small holes are drilled through the walls and if water filled manometers are used to measure the various pressure heads, the results will appear as shown in Figure 6.7 [40, 41, 69].

When a fan blows air through the electronic box, the pressure within the box will be slightly higher than the outside air pressure. A velocity head will now be developed, as shown in Figure 6.8 [40, 41, 69].

The total head will be the sum of the velocity head and the static head, as shown by Eq. 6.3 [40, 41, 69].

$$H_t = H_v + H_s \tag{6.3}$$

When an exhaust fan is used, and the air is drawn through the box, the pressure within the box will be slightly lower than the outside air pressure, and the pressure head characteristics will appear as shown in Figure 6.9. The total head is still shown by Eq. 6.3 [40, 41, 69].

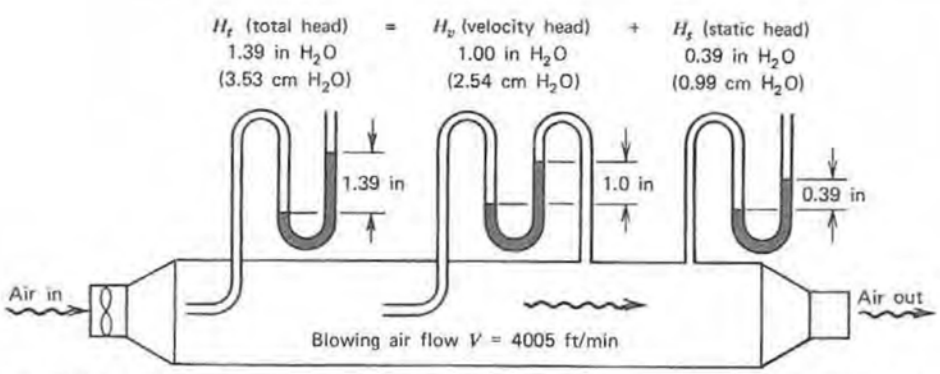

Figure 6.8 Pressure head characteristics when the fan blows air through an electronic box.

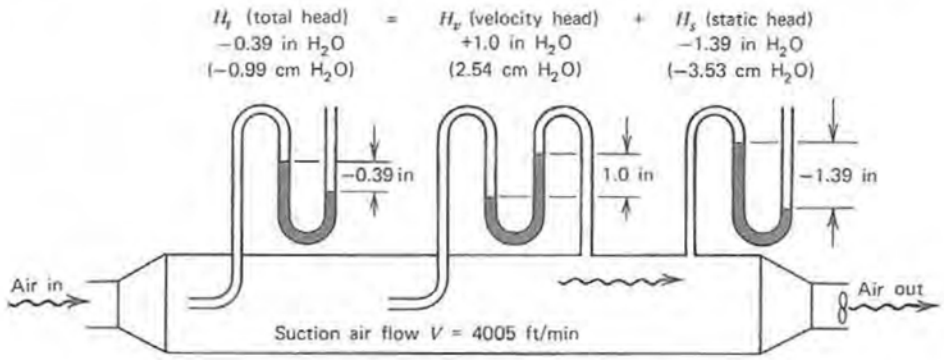

Figure 6.9 Pressure head characteristics when fan draws air through an electronic box.

6.4 LOSSES EXPRESSED IN TERMS OF VELOCITY HEADS

As the cooling air flows through the electronic box, it will experience friction and dynamic losses. There are many ways of expressing these losses. One convenient method is to express the *static* pressure losses in terms of the *velocity* head for the air at some specific point. For example, there will be friction and dynamic losses at the inlets to the fans shown in Figures 6.1 through 6.6. These losses can be expressed as some ratio of the velocity head at the fan inlet. If the loss is judged to be equal to one velocity head, or perhaps two velocity heads for a severely restricted flow area, Eq. 6.2 can be used to determine the actual pressure loss in inches of water, based upon the velocity of the air flow at that section [40, 41, 69].

The loss in a 90° elbow can be expressed as some ratio of the velocity head at that elbow, which is related to the velocity of the air flowing through the elbow. A loss in a sudden expansion is expressed as a ratio of the velocity head just before the expansion. A typical sudden expansion will result in a loss of one velocity head, because the air velocity at the expansion is sharply reduced. Most of the energy required to provide that velocity at the point just before the expansion is lost. That energy was originally supplied by the fan. If more energy is lost, a larger fan is required to supply that energy. If the losses in an air flow system can be reduced, by avoiding such things as sharp turns and sudden expansions, a smaller fan can be used.

Air velocities must be kept low to avoid large losses. High air velocities result in high losses. A system with high losses will require a fan or blower that can supply the required cooling air at a higher pressure. This usually results in a larger and heavier fan or blower, with greater power requirements and higher costs [42].

SEC et al. v. MRI
SEC Exhibit 1027.0184
IPR2023-00255

6.5 SAMPLE PROBLEM—AIR FLOW LOSS AT A FAN ENTRANCE

The axial flow fan shown in Figure 6.1 has an air inlet velocity of 3500 ft/min (1778 cm/sec). It is estimated that the turbulence and contraction in the air at the entrance to the fan will result in a static loss of about 1.5 velocity heads. Determine the static head loss in terms of the height of a column of water.

SOLUTION

The static loss represented by one velocity head can be determined by rewriting Eq. 6.2 slightly, as shown in Eq. 6.4 for English units.

$$H_v = \left(\frac{V}{4005}\right)^2 \tag{6.4}$$

where $V = 3500$ ft/min

$$H_v = \left(\frac{3500}{4005}\right)^2 = 0.764 \text{ in } H_2O \text{ for one velocity head} \tag{6.5}$$

Using Eq. 6.2a for metric units yields

$$H_v = \left(\frac{V}{1277}\right)^2$$

$$H_v = \left(\frac{1778}{1277}\right)^2 = 1.94 \text{ cm } H_2O \text{ for one velocity head} \tag{6.5a}$$

The static head loss at the fan entrance is expected to be 1.5 velocity heads. The static loss expected in English units is shown in Eq. 6.6.

$$H_{\substack{\text{fan}\\\text{loss}}} = 1.5(0.764 \text{ in } H_2O) = 1.146 \text{ in } H_2O \tag{6.6}$$

The static loss expected, in metric units, is shown in Eq. 6.6a.

$$H_{\substack{\text{fan}\\\text{loss}}} = 1.5(1.94 \text{ cm} H_2O) = 2.91 \text{ cm } H_2O \tag{6.6a}$$

The air exit velocity should also be kept low, if possible, to reduce the velocity head lost at the exit. Sometimes a gradual enlargement can be incorporated at the exit. This will help to convert some of the velocity head to a higher static head, which will help to increase the flow of air through the box.

SEC et al. v. MRI
SEC Exhibit 1027.0185
IPR2023-00255

6.6 ESTABLISHING THE FLOW IMPEDANCE CURVE FOR AN ELECTRONIC BOX

Electronic boxes that are cooled with the use of fans must be carefully evaluated to make sure the fan will provide the proper cooling. If the fan is too small for the box, the electronic system may overheat and fail. If the fan is too big for the box, the cooling will be adequate, but the larger fan will be more expensive, heavier, and will draw more power.

Air flowing through the electronic box will encounter resistance as it enters different chambers and is forced to make many turns. This flow resistance is approximately proportional to the square of the velocity, so that it is approximately proportional to the square of the flow rate in cubic foot per minute (cfm). When the static pressure of the air flow through a box is plotted against the cfm air flow rate, the result will be a parabolic curve. This curve can be generated by considering the various flow resistances the moving air will encounter as it flows through the box. The method of analysis is to assume several different cfm flow rates through the box and then to calculate a static pressure drop through the box for each flow rate. The result will be a curve similar to Figure 6.10.

Once the box flow impedance curve has been developed, it is necessary to examine different fan impedance curves to see how well the fans will match the box. A typical fan impedance curve is shown in Figure 6.11.

If the impedance curve for the box is superimposed on the impedance curve for the fan, they will intersect. The point of intersection represents the actual operating point for the system, as shown in Figure 6.12 [42].

The method of pressure drop analysis just outlined can be demonstrated by considering a typical fan cooled electronic box.

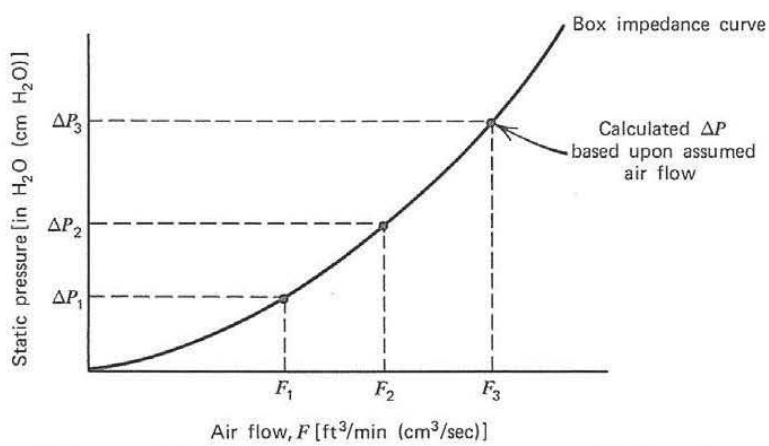

Figure 6.10 Typical air flow impedance curve for an electronic box.

SEC et al. v. MRI
SEC Exhibit 1027.0186
IPR2023-00255

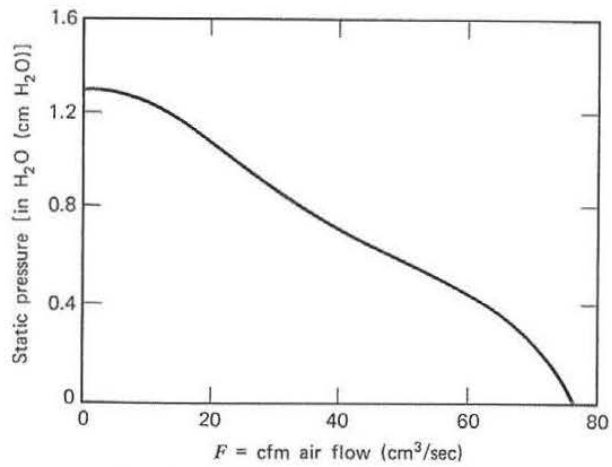

Figure 6.11 Typical flow impedance curve for a fan.

6.7 SAMPLE PROBLEM—FAN COOLED ELECTRONIC BOX

Determine the pressure drop characteristics of the electronic box in Figure 6.13, and determine a fan size for the system. The system must be capable of continuous operation in a 131°F (55°C) ambient at sea level conditions. The maximum allowable hot spot component surface temperature is limited to 212°F (100°C). The system contains seven PCBs, each dissipating 20 watts, for a total power dissipation of 140 watts. This does not include the fan power dissipation.

SOLUTION

The box must be examined in two phases to ensure the integrity of the complete design. In phase 1, the thermal design of the box is examined,

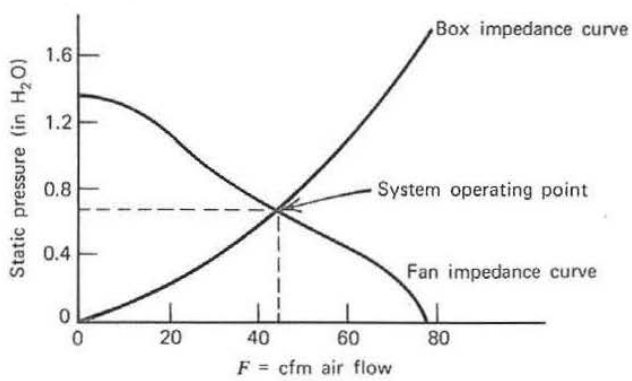

Figure 6.12 Intersection of fan and box impedance curves.

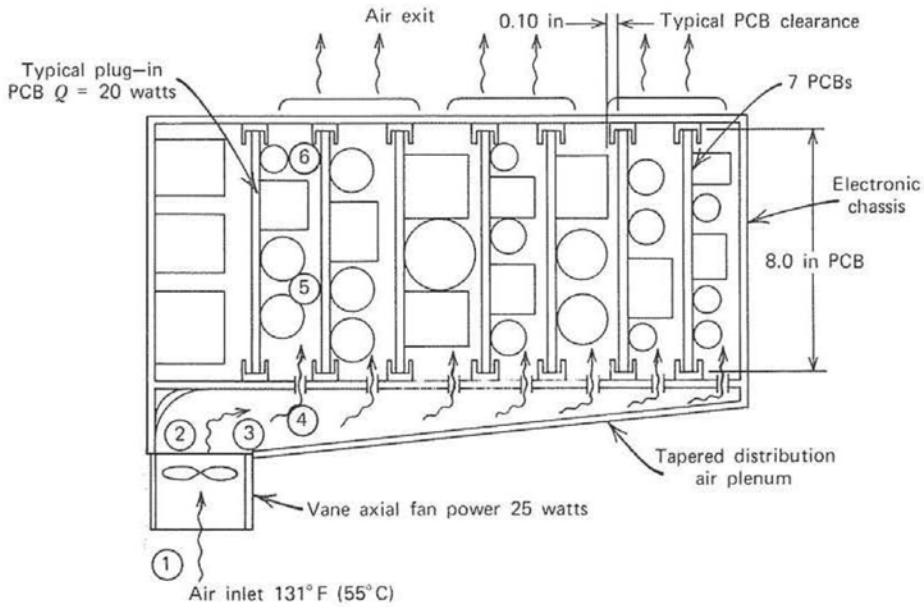

Figure 6.13 Plan view of fan cooled electronic box.

with the proposed fan, to make sure the component hot spot temperature of 212°F (100°C) is not exceeded. In phase 2, the electronic chassis air flow impedance curve is developed and matched with several fans, to make sure there is sufficient cooling air available for the system.

Phase 1. Electronic Box Thermal Design

A preliminary thermal analysis must be made of the system to determine approximately how much cooling air is required. The preliminary analysis can also be used to establish an approximate fan size.

The maximum allowable temperature rise from the air inlet to the component surface hot spot temperature is 212°F − 131°F = 81°F (100°C − 55°C = 45°C). There are two major contributors to this temperature rise.

1 Δt due to the heat input from the fan and the electronics to the cooling air.
2 Δt due to the thermal resistance across the convection film from the cooling air to the surface of the component.

These temperature rise sources can be examined in more detail to see how much each contributes to the total value.

1 Δt due to the heat input from the fan motor to the cooling air.

SEC et al. v. MRI
SEC Exhibit 1027.0188
IPR2023-00255

Heat generated by the fan motor is usually removed by convection from the cooling air. If the fan is bolted to a large heat sink away from the electronic box, a large part of the heat from the fan motor may be removed by direct conduction and radiation from the fan housing to the heat sink.

When the fan is bolted directly to the chassis that houses the electronics, the chassis walls may be quite hot, so relatively little fan heat may be transferred to the chassis. Therefore, it is a good practice to be slightly conservative and to assume that all of the fan power will be picked up by the cooling air as it passes through the fan and into the chassis housing.

Several types of fans can be used for cooling the electronics. Centrifugal fans (sometimes called radial or squirrel cage blowers) can deliver a large quantity of air against a high static pressure. Also, there are probably more centrifugal fans in general use for cooling than any other type of fan. However, centrifugal fans are generally larger and heavier than tube axial and vane axial fans for the same performance in small fan sizes. Axial flow fans will be required to run at higher speeds to get the same performance, so that they will generate more noise than will centrifugal fans.

If a small, high speed axial flow fan is selected, the noise generated may be objectionable to personnel working in areas adjacent to the fan. Simple mufflers can be made of plywood and foam packing material to reduce the noise levels when these fans are operating with room ambient cooling air.

Past experience with air cooled electronic systems has shown that satisfactory thermal performance can be obtained if the cooling air exit temperature from the electronic chassis does not exceed 160°F (71°C). The allowable cooling air temperature rise then becomes

$$\Delta t_A = 160°\text{F} - 131°\text{F} = 29°\text{F}$$

or

$$\Delta t_A = 71°\text{C} - 55°\text{C} = 16°\text{C}$$

The required cooling air weight flow for the system can then be determined from the general weight flow equation [15, 17, 24].

$$W = \frac{Q}{\Delta t C_p} \tag{6.7}$$

Given

Item	*English Units*		*Metric Units*
Q = heat	= Btu/hr	=	cal/sec
Δt = temperature rise	= °F	=	°C
C_p = specific heat	= Btu/lb °F	=	cal/g °C
W = air flow	= lb/hr	=	g/sec

SEC et al. v. MRI
SEC Exhibit 1027.0189
IPR2023-00255

Considering a lightweight vane axial flow fan similar to the Rotron Aximax 2, which weighs only about 0.25 lb, the power dissipation for a 15,000 rpm fan will be about 25 watts, The total box power dissipation in English units then becomes:

$$Q = 140 + 25 = 165 \text{ watts} \times 3.413 \frac{\text{Btu/hr}}{\text{watts}} = 563 \frac{\text{Btu}}{\text{hr}} \text{ (heat)}$$

$$\Delta t = 160 - 131 = 29°\text{F (cooling air temperature rise)}$$

$$C_p = 0.24 \frac{\text{Btu}}{\text{lb °F}} \text{ (specific heat)}$$

The cooling air flow through the box must be

$$W = \frac{563 \text{ Btu/hr}}{(29°\text{F})(60 \text{ min/hr})(0.24 \text{ Btu/lb °F})} = 1.35 \frac{\text{lb}}{\text{min}} \tag{6.8}$$

In metric units:

$$Q = 140 + 25 = 165 \text{ watts} \times 0.239 \frac{\text{cal/sec}}{\text{watt}} = 39.4 \text{ cal/sec (heat)}$$

$$\Delta t = 71 - 55 = 16°\text{C}$$

$$C_p = 0.24 \frac{\text{cal}}{\text{g °C}} \text{ (specific heat)}$$

$$W = \frac{39.4 \text{ cal/sec}}{(16°\text{C})(0.24 \text{ cal/g °C})} = 10.3 \frac{\text{g}}{\text{sec}} \tag{6.8a}$$

2 Δt due to the thermal resistance across the convection film from the cooling air to the surface of the component.

This temperature rise can be determined from the convection relation shown by Eq. 5.7.

$$\Delta t = \frac{Q}{h_c A} \qquad \text{(ref. Eq. 5.7)}$$

The convection coefficient h_c is determined from the geometry of the air duct that is formed by the air space between the plug-in PCBs. Its value is determined from Eq. 6.9 [3, 15, 43].

$$h_c = JC_pG\left(\frac{C_p\mu}{K}\right)^{-2/3} \tag{6.9}$$

SEC et al. v. MRI
SEC Exhibit 1027.0190
IPR2023-00255

Given J = Colburn factor
C_p = specific heat of fluid (ref. Figure 6.28)
G = weight velocity flow through duct
μ = viscosity of fluid (ref. Figure 6.28)
K = thermal conductivity of fluid (ref. Figure 6.28)

The Colburn J factor can be determined from the Reynolds number (N_R). For laminar flow conditions with N_R between 200 and 1800, the approximate J value for rectangular ducts with aspect ratios greater than about 8 is shown in Eq. 6.10 (compiled from data shown in Kays and London, *Compact Heat Exchangers*) [43].

$$J = \frac{6}{(N_R)^{0.98}} \tag{6.10}$$

For square ducts (aspect ratio = 1.0) the approximate J value for the same laminar flow conditions is as follows:

$$J = \frac{2.7}{(N_R)^{0.95}} \tag{6.10a}$$

For turbulent conditions, where N_R is between 10,000 and 120,000 McAdams [15] shows that

$$J = \frac{0.023}{(N_R)^{0.2}} \tag{6.10b}$$

The air duct formed by the clearance between the components and the PCBs is shown in Figure 6.14.

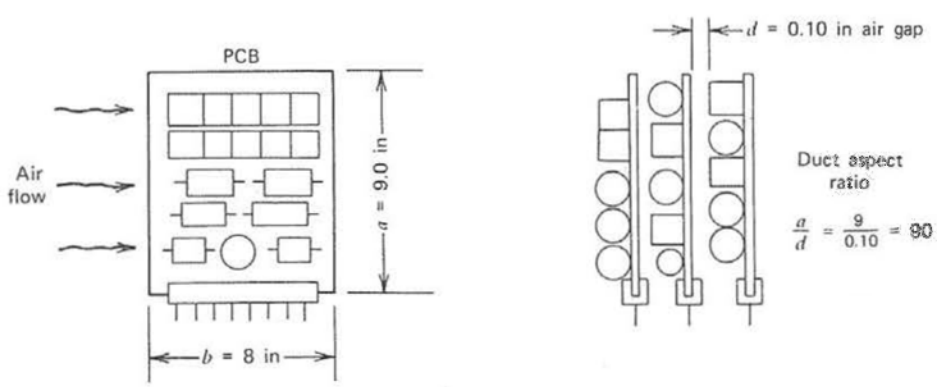

Figure 6.14 Air flow duct formed between printed circuit boards.

The Reynolds number for the air duct formed by the PCBs is shown in Eq. 6.11.

$$N_R = \frac{VD\rho}{\mu} = \frac{GD}{\mu} \tag{6.11}$$

Given $D = \dfrac{4 \times \text{area}}{\text{perimeter}} = \dfrac{4ad}{2(a+d)} = \dfrac{2ad}{a+d}$ (hydraulic diameter)

In English units:

$$D = \frac{2(9.0)(0.10)}{9.0 + 0.10} = 0.198 \text{ in} = 0.0165 \text{ ft}$$

In metric units:

$$D = \frac{2(22.86)(0.254)}{22.86 + 0.254} = 0.502 \text{ cm}$$

The weight velocity flow G through the duct formed by the PCBs is determined from Eq. 6.12.

$$G = \frac{W}{A} \tag{6.12}$$

Given $W = 1.35$ lb/min (10.3 g/sec) (ref. Eq. 6.8)

$$A = \frac{(9.0)(0.10) \text{ in}^2}{144 \text{ in}^2/\text{ft}^2} = 0.00625 \text{ ft}^2 \text{ (area one duct)}$$

In English units:

$$G = \frac{(1.35 \text{ lb/min})(60 \text{ min/hr})}{0.00625 \text{ ft}^2 \times 7 \text{ ducts}} = 1851 \frac{\text{lb}}{\text{hr ft}^2} \tag{6.13}$$

In metric units:

$$G = \frac{10.3 \text{ g/sec}}{(22.86)(0.254) \text{ cm}^2 \times 7 \text{ ducts}} = 0.253 \frac{\text{g}}{\text{sec cm}^2} \tag{6.13a}$$

$$\mu = 0.050 \frac{\text{lb}}{\text{ft hr}} = 0.000207 \frac{\text{g}}{\text{cm sec}} \text{ [ref. Fig. 6.28; viscosity at 150°F (65.5°C)]}$$

SEC et al. v. MRI
SEC Exhibit 1027.0192
IPR2023-00255

Substitute into Eq. 6.11 for the Reynolds number, in English units:

$$N_R = \frac{(1851 \text{ lb/hr ft}^2)(0.0165 \text{ ft})}{0.050 \text{ lb/ft hr}} = 611 \text{ (dimensionless)} \tag{6.14}$$

In metric units:

$$N_R = \frac{(0.253 \text{ g/sec cm}^2)(0.502 \text{ cm})}{0.000207 \text{ g/cm sec}} = 613 \text{ (dimensionless)} \tag{6.14a}$$

$$K = 0.017 \frac{\text{Btu}}{\text{hr ft °F}} = 0.000070 \frac{\text{cal}}{\text{sec cm °C}} \text{ (ref. Fig. 6.28; thermal conductivity at 150°F)}$$

Substitute into Eq. 6.10 for the J factor.

$$J = \frac{6}{(N_R)^{0.98}} = \frac{6}{(611)^{0.98}} = 0.0111 \text{ (dimensionless)}$$

Substitute into Eq. 6.9 for the forced air convection coefficient, in English units.

$$h_c = \frac{(0.0111)(0.24)(1851 \text{ lb/hr ft}^2)}{[(0.24 \times 0.05)/0.017]^{0.666}} = 6.22 \frac{\text{Btu}}{\text{hr ft}^2 \text{ °F}} \tag{6.15}$$

In metric units:

$$h_c = \frac{(0.0111)(0.24)(0.253 \text{ g/sec cm}^2)}{[(0.24 \times 0.000207)/0.000070]^{0.666}} = 0.000846 \frac{\text{cal}}{\text{sec cm}^2 \text{ °C}} \tag{6.15a}$$

Section 5.11 points out that some of the surface area on the backside of flow soldered PCBs is available for heat dissipation when the component lead wires extend through the PCB. When there is copper on the back side of such a PCB, the heat can flow through the PCB to the copper, which acts as a heat spreader. As much as 30% of the back side of a PCB may be available for effective heat transfer. The total heat transfer surface area may then be 1.3 times the area of one face on the PCB.

The forced convection coefficient h_c can be increased by using a smaller air gap between the PCBs. For example, if the air gap is reduced from 0.10 in to 0.08 in, the forced convection coefficient will increase to a value of about 7.8 Btu/hr ft² °F. However, if the electronic system must operate in a severe vibration environment, there must be sufficient sway space between the PCBs, to prevent tall electronic components from striking the sharp lead wires on the back surface of the adjacent PCB.

The temperature rise across the convection film from the air stream to

SEC et al. v. MRI
SEC Exhibit 1027.0193
IPR2023-00255

the component surface can now be determined using Eq. 5.7. The heat from the fan is not included with the heat generated by the PCBs. Each PCB dissipates 20 watts = 68.3 Btu/hr.

Given $Q = 68.3$ Btu/hr = 4.78 cal/sec (heat)
$h_c = 6.22$ Btu/hr ft^2 °F = 0.000846 cal/sec cm^2 °C (convection)

In English units:

$$A = \frac{(1.3)(8)(9)\ \text{in}^2}{144\ \text{in}^2/\text{ft}^2}$$

$$= 0.65\ \text{ft}^2 \text{ (PCB area, including the back side of the PCB)}$$

In metric units:

$$A = (1.3)(20.32)(22.86) = 603.8\ \text{cm}^2 \text{ (PCB area)}$$

The temperature rise, in English units, is

$$\Delta t_B = \frac{68.3}{(6.22)(0.65)} = 16.9°\text{F} \tag{6.16}$$

In metric units:

$$\Delta t_B = \frac{4.78}{(0.000846)(603.8)} = 9.3°\text{C} \tag{6.16a}$$

The component hot spot surface temperature t_s is determined from the cooling air inlet temperature, plus the temperature rises to the component surface, as shown in Eq. 6.17.

$$t_s = t_{\text{in}} + \Delta t_A + \Delta t_B \tag{6.17}$$

In English units, the component surface temperature is

$$t_s = 131 + 29 + 16.9 = 176.9°\text{F} \tag{6.18}$$

In metric units:

$$t_s = 55 + 16 + 9.3 = 80.3°\text{C} \tag{6.18a}$$

Since the component hot spot surface temperature is less than 212°F (100°C), the initial design concept with the vane axial flow fan appears to be satisfactory.

SEC et al. v. MRI
SEC Exhibit 1027.0194
IPR2023-00255

Phase 2. Electronic Chassis Air Flow Impedance Curve

The air flow conditions are examined at six different points in the chassis, where the maximum static pressure losses are expected to occur, as shown in Figure 6.13. These static pressure losses are itemized as follows:

1 Air inlet to fan
2 90° turn and transition to an oval section
3 Contraction and transition to a rectangular section
4 Plenum entrance to PCB duct
5 Flow through PCB channel duct
6 Exhaust from PCB duct and chassis

The static pressure losses are examined in greater detail using the velocity head loss technique discussed in Section 6.4.

1 *Air Inlet to Fan.* The air inlet to the axial flow fan is very similar to the plain end duct, as shown in Table 6.2 (Section 6.12). Ducts of this type can be expected to show a static pressure loss of 0.93 velocity head. The loss is conservatively rounded off to 1.0 velocity head, as shown in Eq. 6.19.

$$H_1 = 1.0H_{v1} \tag{6.19}$$

2 *90° Turn and Transition from a Round Section at the Fan to an Oval Section.* The radius of the turn is rather sharp, probably less than 1 diameter. Also, the section is changing from round to oval (the section will eventually become rectangular).

$$\begin{aligned} 90° \text{ turn} &= 0.7\,H_v \\ \text{Transition} &= \underline{0.2\,H_v} \\ &\ 0.9\,H_v \end{aligned}$$

Conservatively round off this loss to unity.

$$H_2 = 1.0H_{v2} \tag{6.20}$$

3 *Contraction and Transition to Rectangular Section*

$$\begin{aligned} \text{Contraction} &= 0.2H_v \\ \text{Transition} &= \underline{0.2H_v} \\ &\ 0.4H_v \end{aligned}$$

SEC et al. v. MRI
SEC Exhibit 1027.0195
IPR2023-00255

Conservatively round off to $0.5H_v$.

$$H_3 = 0.5H_{v3} \tag{6.21}$$

4 *Plenum Entrance to Printed Circuit Board (PCB) Duct.* The air must make an abrupt change at this point. It must make a 90° turn and enter the PCB duct area. This is a critical area with respect to pressure drop. If the inlet extends slightly into the air stream, as shown in Figure 6.15*a*, the pressure loss can exceed 3 velocity heads as a result of the turbulence generated ($2.7H_v$ entry + $1.0H_v$ for 90° turn = $3.7H_v$ total loss) [41, 69].

An attempt should be made to keep the entrance flush. It is much better to bevel the edges as shown in Figure 6.15*b*, where the pressure loss is only about 1.5 velocity heads ($0.5H_v$ entry + $1.0H_v$ turn = $1.5H_v$ total loss).

Conservatively assume a flush edge.

$$\begin{aligned} \text{Entrance} &= 1.0H_v \\ 90^\circ \text{ turn} &= 1.0H_v \\ \hline H_4 &= 2.0H_{v4} \end{aligned} \tag{6.22}$$

5 *Air Flow through PCB Channel Duct.* In this case the duct is really the space between the backside of one board and the electronic components on the adjacent board. The back side of the PCB has small exposed tips of the electrical lead wires, and the front side of the PCB is populated with electronic components. The loss can be expressed in terms of air flowing through a rectangular duct as shown in Section 6.24 (Eq. 6.82 or 6.83). Using velocity heads for convenience, a high pressure loss is expected for this condition because of the narrow (0.10 in) air gap.

$$H_5 = 1.0H_{v5} \tag{6.23}$$

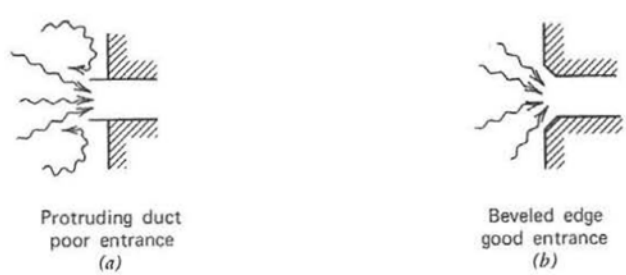

Figure 6.15 Protruding duct creates turbulence that increases pressure loss at air inlet (*a*); beveled edge reduces pressure loss at air inlet (*b*).

SEC et al. v. MRI
SEC Exhibit 1027.0196
IPR2023-00255

6 *Exhaust from PCB Duct and Chassis.* This calculation is normally not included in the static pressure drop loss through the box. However, it is always a good idea to see how much energy is being thrown away at the exit. Remember that the fan must supply all of the air-moving energy. If too much is thrown away at the exhaust, the fan has to work harder. When the exhaust loss is too high in a critical design, some attempt should be made to recover part of the loss by slightly enlarging the exhaust area to reduce the exhaust velocity.

As the cooling air exhausts from the box, it will expand suddenly, so that it will lose its velocity completely.

$$H_6 = 1.0H_{v6} \tag{6.24}$$

Note that the air flows across all of the PCBs in a parallel flow path. The pressure drop across this section will all be about the same for all of the PCBs. Therefore, only one air flow path across the circuit board stack has to be examined to obtain the pressure drop.

All of the information is now available to calculate the approximate pressure drop through the box based upon the geometry of the air flow path. Three different cfm air flow conditions will be assumed: 10 cfm (4719 cm³/sec), 20 cfm (9438 cm³/sec), and 30 cfm (14157 cm³/sec). The pressure drops at each of the six points in Figure 6.13 will be determined for each of the three assumed flow conditions, starting with the 10 cfm (4719 cm³/sec) flow condition.

1 *Air Inlet to Fan.* Equation 6.4 shows that the velocity head H_v is a function of the air flow velocity in feet per minute. Starting with an assumed air flow of 10 cfm, the cross section flow area through the axial flow fan is required, and is shown in Figure 6.16.

$$A_1 = \frac{(\pi/4)[(1.88)^2 - (1.10)^2]\ \text{in}^2}{144\ \text{in}^2/\text{ft}^2} = 0.0127\ \text{ft}^2 = 11.8\ \text{cm}^2$$

$$V_1 = \frac{F}{A_1} = \frac{10\ \text{ft}^3/\text{min}}{0.0127\ \text{ft}^2} = 787\ \frac{\text{ft}}{\text{min}} = 400\ \frac{\text{cm}}{\text{sec}}$$

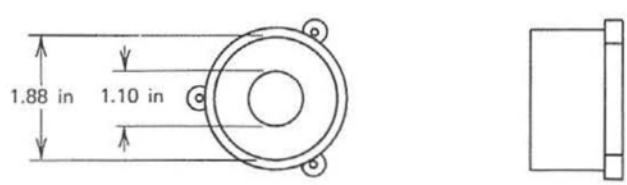

Figure 6.16 Cross section flow area for a small lightweight vane axial flow fan (similar to Rotron Aximax 2).

SEC et al. v. MRI
SEC Exhibit 1027.0197
IPR2023-00255

Substitute into Eq. 6.4 for the velocity head at point 1 in English units.

$$H_{v1} = \left(\frac{V}{4005}\right)^2 = \left(\frac{787}{4005}\right)^2 = 0.0386 \text{ in } H_2O \tag{6.25}$$

In metric units:

$$H_{v1} = \left(\frac{V}{1277}\right)^2 = \left(\frac{400}{1277}\right)^2 = 0.098 \text{ cm } H_2O \tag{6.25a}$$

The losses for each flow rate of 10 cfm, 20 cfm, and 30 cfm can be determined from Eq. 6.19 by using a ratio of the 10 cfm flow rate.

$$\left.\begin{aligned}
&10 \text{ cfm:} \quad H_1 = (1.0)(0.0386) = 0.0386 \text{ in } H_2O = 0.098 \text{ cm } H_2O \\
&20 \text{ cfm:} \quad H_1 = \left(\frac{20}{10}\right)^2 (0.0386) = 0.1544 \text{ in } H_2O = 0.392 \text{ cm } H_2O \\
&30 \text{ cfm:} \quad H_1 = \left(\frac{30}{10}\right)^2 (0.0386) = 0.3474 \text{ in } H_2O = 0.882 \text{ cm } H_2O
\end{aligned}\right\} \tag{6.26}$$

2 *90° Turn and Transition from a Round Section at the Fan to an Oval Section.* The cross section area at section 2 is shown in Figure 6.17.

$$A_2 = \frac{(\pi/4)(0.5)^2 + (3.5)(0.5) \text{ in}^2}{144 \text{ in}^2/\text{ft}^2} = 0.0135 \text{ ft}^2 = 12.56 \text{ cm}^2$$

$$V_2 = \frac{10 \text{ ft}^3/\text{min}}{0.0135 \text{ ft}^2} = 741 \frac{\text{ft}}{\text{min}} = 376 \frac{\text{cm}}{\text{sec}}$$

Substitute into Eq. 6.4 for the velocity head at point 2.

$$H_{v2} = \left(\frac{741}{4005}\right)^2 = 0.034 \text{ in } H_2O = 0.087 \text{ cm } H_2O$$

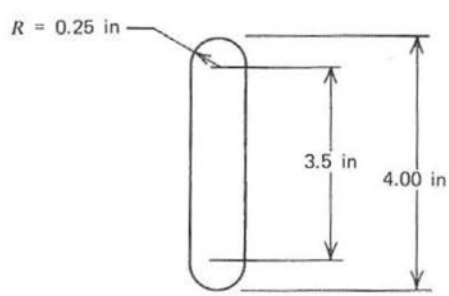

Figure 6.17 Cross section of air flow path at point 2.

SEC et al. v. MRI
SEC Exhibit 1027.0198
IPR2023-00255

The losses for each flow rate at point 2 are determined from Eq. 6.20.

$$\left.\begin{aligned}
&10\text{ cfm:}\quad H_2 = (1.0)(0.034) = 0.034\text{ in H}_2\text{O} = 0.086\text{ cm H}_2\text{O}\\
&20\text{ cfm:}\quad H_2 = \left(\frac{20}{10}\right)^2(0.034) = 0.136\text{ in H}_2\text{O} = 0.345\text{ cm H}_2\text{O}\\
&30\text{ cfm:}\quad H_2 = \left(\frac{30}{10}\right)^2(0.034) = 0.306\text{ in H}_2\text{O} = 0.777\text{ cm H}_2\text{O}
\end{aligned}\right\}\quad(6.27)$$

3 *Contraction and Transition to Rectangular Section.* The cross section area at section 3 is shown in Figure 6.18.

$$V_3 = \frac{10\text{ cfm}}{0.0104} = 961\,\frac{\text{ft}}{\text{min}} = 488\,\frac{\text{cm}}{\text{sec}}$$

$$H_{v3} = \left(\frac{961}{4005}\right)^2 = 0.0575\text{ in H}_2\text{O} = 0.146\text{ cm H}_2\text{O}$$

The losses for each flow rate at point 3 are determined from Eq. 6.21.

$$\left.\begin{aligned}
&10\text{ cfm:}\quad H_3 = (0.5)(0.0575) = 0.0287\text{ in H}_2\text{O} = 0.0729\text{ cm H}_2\text{O}\\
&20\text{ cfm:}\quad H_3 = \left(\frac{20}{10}\right)^2(0.0287) = 0.115\text{ in H}_2\text{O} = 0.292\text{ cm H}_2\text{O}\\
&30\text{ cfm:}\quad H_3 = \left(\frac{30}{10}\right)^2(0.0287) = 0.259\text{ in H}_2\text{O} = 0.657\text{ cm H}_2\text{O}
\end{aligned}\right\}\quad(6.28)$$

4 *Plenum Entrance to PCB Duct.* The cross section at section 4 is shown in Figure 6.19. Since there are seven card slots, approximately $\frac{1}{7}$ of the total flow will pass through each slot if the tapered distribution duct shown in Figure 6.13 does its job properly. When the power dissipation is not the same on each PCB, more air should be distributed to the PCBs that have a higher power dissipation. A mockup of the

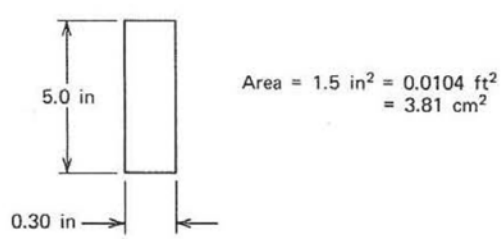

Figure 6.18 Cross section of air flow path at point 3.

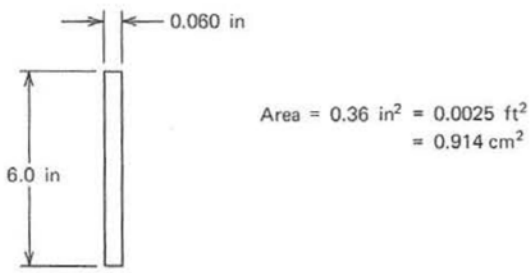

Figure 6.19 Inlet slot for distributing cooling air to PCB duct.

air flow system is usually built and tested, to make sure the air distribution to each PCB is adequate.

$$V_4 = \frac{10 \text{ cfm}}{(0.0025 \text{ ft}^2)(7 \text{ slots})} = 571 \frac{\text{ft}}{\text{min}} = 290 \frac{\text{cm}}{\text{sec}}$$

$$H_{v4} = \left(\frac{571}{4005}\right)^2 = 0.0203 \text{ in } H_2O = 0.0516 \text{ cm } H_2O$$

The losses for each flow rate at point 4 are determined from Eq. 6.22.

$$\left.\begin{aligned} &10 \text{ cfm:} \quad H_4 = (2)(0.0203) = 0.0406 \text{ in } H_2O = 0.103 \text{ cm } H_2O \\ &20 \text{ cfm:} \quad H_4 = \left(\frac{20}{10}\right)^2 (0.0406) = 0.162 \text{ in } H_2O = 0.411 \text{ cm } H_2O \\ &30 \text{ cfm:} \quad H_4 = \left(\frac{30}{10}\right)^2 (0.0406) = 0.365 \text{ in } H_2O = 0.927 \text{ cm } H_2O \end{aligned}\right\} \quad (6.29)$$

5 Air Flow through PCB Channel Duct. The cross section of the duct formed by the PCBs is shown in Figure 6.14.

$$A_5 = (0.10)(9.0) = 0.90 \text{ in}^2 = 0.00625 \text{ ft}^2 = 5.80 \text{ cm}^2$$

$$V_5 = \frac{10 \text{ cfm}}{(0.00625 \text{ ft}^2)(7 \text{ slots})} = 228 \frac{\text{ft}}{\text{min}} = 116 \frac{\text{cm}}{\text{sec}}$$

$$H_{v5} = \left(\frac{228}{4005}\right)^2 = 0.0032 \text{ in } H_2O = 0.0082 \text{ cm } H_2O$$

The losses for each flow rate at point 5 are determined from Eq. 6.23.

SEC et al. v. MRI
SEC Exhibit 1027.0200
IPR2023-00255